Cookstoves, Candles, and Phthalates – Real Time Physicochemical Characterization and Human Exposure to Indoor Aerosols

Andersen, Christina

2021

Document Version:
Publisher's PDF, also known as Version of record

Link to publication

Citation for published version (APA):
Andersen, C. (2021). *Cookstoves, Candles, and Phthalates – Real Time Physicochemical Characterization and Human Exposure to Indoor Aerosols*. Division of Ergonomics and Aerosol Technology, Department of Design Sciences Lund University.

Total number of authors:
1

LUND UNIVERSITY

PO Box 117
221 00 Lund
+46 46-222 00 00

Cookstoves, Candles, and Phthalates
– Real Time Physicochemical Characterization and Human Exposure to Indoor Aerosols

CHRISTINA ANDERSEN
ERGONOMICS AND AEROSOL TECHNOLOGY | LTH | LUND UNIVERSITY

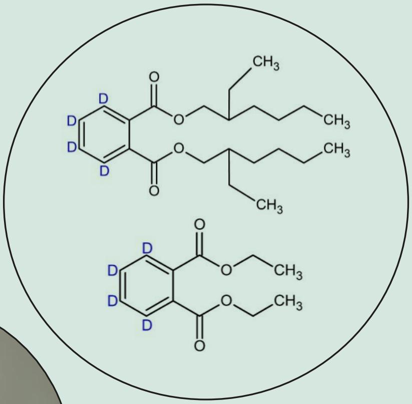

Cookstoves, Candles, and Phthalates – Real Time Physicochemical Characterization and Human Exposure to Indoor Aerosols

Christina Andersen

LUND
UNIVERSITY

DOCTORAL DISSERTATION

by due permission of the Faculty of Engineering, Lund University, Sweden.
To be defended at Stora Hörsalen, IKDC. Date 2021-05-12 and time 14:15.

Faculty Opponent
Associate Professor Delphine Farmer
Colorado State University, USA

Organization LUND UNIVERSITY	**Document name** Doctoral Dissertation
	Date of issue 2021-05-12
Author Christina Andersen	Sponsoring organization

Title and subtitle Cookstoves, Candles, and Phthalates – Real Time Physicochemical Characterization and Human Exposure to Indoor Aerosols

Abstract

Exposure to air pollution is associated with adverse health effects in humans, with special concern for exposure to fine particulate matter ($PM_{2.5}$). The physicochemical properties of aerosols impact the health effects. Considering that we spend approximately 90% of our time indoors, it is important to gain increased understanding of indoor aerosol concentrations and properties. The overall aim of the research presented in this thesis was to characterize the physicochemical properties of indoor aerosols from cookstoves, candles, and phthalate sources, and to assess their contribution to human exposure. Aerosol mass spectrometry (AMS) was applied for real time measurements of the aerosol chemical composition and concentration throughout the measurements included in the thesis.

Emissions from four different cookstoves commonly used in sub Saharan Africa were measured with AMS and interpreted on the basis of a simplified framework describing the thermochemical conversion of biomass. The framework was validated by a correlation analysis of the included emission classes. Moreover, the results showed reduced PM_1 emissions for more advanced stoves. However, pollutants which are of specific health concern, were not reduced in proportion to PM_1. Even when PM_1 emissions were reduced, high emissions of pollutants that have a strong impact on health and climate may be emitted, for example polycyclic aromatic compounds (PAHs) and refractory black carbon (rBC). The framework may be applied to estimate emissions of classes that were not measured in the experiments.

Aerosol emissions from stressed burning of five types of candles of different wax and wick compositions were studied. We found strong variations between the candle types in emissions of $PM_{2.5}$, BC, and PAHs, as well as strong variations over time, depending on the wax and wick composition. Candle emissions from stressed burning were dominated by BC emissions, with minor contributions from inorganic and organic aerosol emissions. The candles that emitted the lowest BC concentrations showed high emissions of ultrafine particles. NO_x, formaldehyde, and gas-phase PAHs showed less variation between candle types and proved difficult to reduce by altering the wax and wick composition. The emissions of particle phase PAHs, BC, and organic aerosol showed strong correlations at the stressed burning of candles, and may be used as proxies for each other.

The sorption of di-(2-ethyhexyl) phthalate (DEHP) on laboratory generated ammonium sulfate particles and indoor air particles was investigated by passing the particles through a 1.2 L chamber equipped with polyvinyl chloride (PVC) flooring. A higher sorption of DEHP to indoor particles, with a higher organic mass fraction, was measured compared to laboratory generated ammonium sulfate particles. In presence of airborne particles the emission of DEHP from PVC flooring increased. Thus, when particles are present in indoor air, the airborne concentration of DEHP available for respiratory deposition may increase. The sorption of DEHP on particles depends on the particle chemical composition. Organic particle concentrations are often high indoors, which promotes the sorption of DEHP and other SVOCs, which in turn may contribute to increased human exposure to DEHP and other SVOCs. This highlights the need to reduce health detrimental chemicals in consumer products and building materials, and to reduce particle concentrations in indoor environments.

A human exposure study was conducted to elucidate the dermal and inhalation uptake in 16 volunteers from exposure to airborne gas- and particle phase phthalates, with participants wearing clean clothing. The uptake was measured, via combined inhalation and dermal air-to-skin transfer and via air-to-skin transfer only for the gas-phase diethyl phthalate (DEP) and for particle phase DEHP. Dermal uptake via air-to-skin transfer only with clean clothing acting as a barrier was ten times lower than the uptake via inhalation for DEP. Only uptake via inhalation was measurable for the particle phase DEHP. DEHP uptake via the skin was below the detection limit. The uptake of the gas-phase DEP via inhalation was four times higher compared to the particle phase DEHP, which reflects the differences in the lung deposition of gases and particles. The physicochemical properties of SVOCs influence their gas-particle partitioning and the likelihood of uptake via both inhalation and the skin, which should be considered in risk assessments of SVOCs.

The results presented in this thesis highlight the importance of detailed physicochemical characterization of indoor aerosols, and the need for a more complete evaluation of their impact on human health.

Key words Aerosol particles, OA, BC, cookstoves, candle emissions, phthalates, human exposure, PAHs

ISSN and key title: 1650-9773 Publication 69		**ISBN** 978-91-7895-810-8 (print) **ISBN** 978-91-7895-809-2 (pdf)
Recipient's notes	**Number of pages** 84	Price

I, the undersigned, being the copyright owner of the abstract of the above-mentioned dissertation, hereby grant to all reference sources permission to publish and disseminate the abstract of the above-mentioned dissertation.

Signature Christina Andersen Date 2021-03-30

Cookstoves, Candles, and Phthalates – Real Time Physicochemical Characterization and Human Exposure to Indoor Aerosols

Christina Andersen

LUND
UNIVERSITY

Coverphoto by Christina Andersen

Faculty of Engineering
Department of Design Sciences
Ergonomics and Aerosol Technology (EAT)
Lund University

ISBN 978-91-7895-809-2 (pdf)
ISBN 978-91-7895-810-8 (print)
ISSN 1650-9773 Publication 69

Printed in Sweden by Media-Tryck, Lund University
Lund 2021

NORDIC SWAN ECOLABEL
Printed matter
3041 0903

Media-Tryck is an environmentally
certified and ISO 14001:2015 certified
provider of printed material.
Read more about our environmental
work at www.mediatryck.lu.se

MADE IN SWEDEN

Table of Contents

Papers Included in this Thesis

I) **Andersen, C.**, Lindgren, R. , Eriksson, A.C., Malmborg, V.B., Carvalho, R.L., García-López, N., Ahlberg, E., Falk, J., Kristensen, T.B., Svenningsson, B., Boman, C., & Pagels, J. **Time-Resolved Chemical Composition of Aerosol Emissions from Cookstoves Interpreted on the Basis of a Simplified Thermochemical Conversion Framework**

Manuscript to be submitted for publication

II) **Andersen, C.**, Omelekhina, Y., Rasmussen, B., Nygaard-Bennekov, M., Skov, S. N., Køcks, M., Wang, K., Strandberg, B., Mattsson, F., Bilde, M., Glasius, M., Pagels, J., & Wierzbicka, A. **Emissions of Soot, PAHs, Ultrafine Particles, NO_x, and Other Health Relevant Compounds from Stressed Burning of Candles in Indoor Air**

Submitted to a Scientific Journal

III) Eriksson, A. C., **Andersen, C.**, Krais, A.M., Nojgaard, J. K., Clausen, P. A., Gudmundsson, A., Wierzbicka, A., & Pagels, J. (2020). **Influence of Airborne Particles' Chemical Composition on SVOC Uptake from PVC Flooring – Time-Resolved Analysis with Aerosol Mass Spectrometry**. *Environmental Science & Technology*, 54(1), 85-91.

IV) **Andersen, C.**, Krais, A. M., Eriksson, A. C., Jakobsson, J., Löndahl, J., Nielsen, J., Lindh, C. H., Pagels, J., Gudmundsson, A., & Wierzbicka, A. (2018). **Inhalation and Dermal Uptake of Particle and Gas-phase Phthalates - A Human Exposure Study**. *Environmental Science & Technology*, 52(21), 12792-12800.

Author's Contributions

I) I carried out the majority of the AMS measurements and analyzed the majority of the resulting data included in Paper I. I wrote the major part of the manuscript.

II) I had a major role in designing and planning the measurements, preparatory testing- and in conducting the measurements. I analyzed and interpreted the majority of the data and wrote the major part of Paper II.

III) I conducted and contributed to the optimization of the experiments on the laboratory-generated ammonium sulfate particles, and I analyzed the resulting AMS data. I took part in editing in the writing process and wrote parts of the reply to the reviewers.

IV) I optimized the gas and particle generation in the chamber, and was responsible for the generation of both particle and gas-phase phthalates during the exposures in order to obtain stable exposure concentrations. I was primarily responsible for the generation and the measurements during the exposures. I analyzed and interpreted the online particle measurements, and applied the MPPD model to calculate the deposited dose. I did all the calculations of uptake and excretion factors and wrote the manuscript with comments from the co-authors.

Peer-reviewed Articles Not Included in the Thesis

Rasmussen, B. B., Wang, K., Karstoft, J. G., Skov, S. N., Køcks, M., **Andersen, C**., Wierzbicka, A., Pagels, J., Pedersen, P.B., Glasius, M. and Bilde, M. (2021), **Emissions of Ultrafine Particles from Five Types of Candles during Steady Burn Conditions.** *Indoor Air*. https://doi.org/10.1111/ina.12800

Korhonen, K., Kristensen, T.B., Falk, J., Lindgren, R., **Andersen, C**., Carvalho, R.L., Malmborg, V., Eriksson, A., Boman, C., Pagels, J., Svenningsson, B., Komppula, M., Lehtinen, K.E.J. & Virtanen, A. (2020). **Ice-nucleating Ability of Particulate Emissions from Solid-biomass-fired Cookstoves: An Experimental Study**. *Atmospheric Chemistry & Physics*, 20(8).

Krais, A.M., **Andersen, C.**, Eriksson, A., Johnsson, E., Nielsen, J., Pagels, J., Gudmundsson, A., Lindh, C.H., & Wierzbicka, A. (2018). **Excretion of Urinary Metabolites of the Phthalate Esters DEP and DEHP in 16 Volunteers after Inhalation and Dermal Exposure.** *International Journal of Environmental Research and Public Health*, 15(11), 2514.

Ausmeel, S., **Andersen, C.**, Nielsen, O.J., Østerstrøm, F.F., Johnson M.S., and Nilsson, E.J.K. (2017). **Reactions of Three Lactones with Cl, OD, and O3: Atmospheric Impact and Trends in Furan Reactivity**. *The Journal of Physical Chemistry A*, 121(21), 4123-4131.

Andersen, C., Nielsen, O.J., Østerstrøm, F.F., Ausmeel, S., Nilsson, E.J., & Sulbaek Andersen, M.P. (2016). **Atmospheric Chemistry of Tetrahydrofuran, 2-Methyltetrahydrofuran, and 2, 5-Dimethyltetrahydrofuran: Kinetics of Reactions with Chlorine Atoms, OD Radicals, and Ozone**. *The Journal of Physical Chemistry A*, 120(37), 7320-7326.

Martinsson, J., Eriksson, A.C., Elbæk Nielsen, I., Berg Malmborg, V., Ahlberg, E., **Andersen, C.**, Lindgren, R., Nyström, R., Nordin, E. Z., Brune, W.H, Svenningsson, B., Swietlicki, E., Boman, C., & Pagels, J.H. (2015). **Impacts of Combustion Conditions and Photochemical Processing on the Light Absorption of Biomass Combustion Aerosol**. *Environmental Science & Technology*, 49(24), 14663-14671.

Popular Science Summary

The air we breathe contains small amounts of liquid and solid particles suspended in gas, altogether called aerosols. The sources of aerosol particles are both natural and human made, and they are essential for our climate. They affect cloud formation, the incoming solar light (radiation), and the radiation reflected back to space, thereby influencing Earth's radiative balance. Aerosol particles also impact human health negatively. Upon inhalation, some particles deposit in our lungs and can even be distributed to other organs. Nine out of ten of the world's population breathe air that does not live up to the air pollution guidelines set by the World Health Organization (WHO). Developing countries are experiencing the highest burden of increased air pollution levels.

The aim of the research presented in this thesis was to gain increased knowledge of characteristics of the emissions from common indoor aerosol sources, including cookstoves and candles, with a focus on emissions relevant to health and climate. An additional aim was to investigate the uptake of phthalates (hormone disrupting compounds) on different particle types, and to study how airborne phthalates are taken up in our bodies by conducting a human exposure study.

One of the main sources of household air pollution in developing countries is the use of simple biomass stoves for cooking and heating. A large variety of cookstoves are on the market, ranging from the traditional and most widely used 3-stone fire, which is an open fire between three stones, to improved and advanced stoves, where the insulation and more controlled air supply have been incorporated into the stove design. In this thesis research, the pollutant emissions from four different cookstoves were characterized chemically by using real time measurements. The traditional 3-stone fire showed the highest total aerosol mass concentration per kilo burned fuel. Concentrations decreased with the increasing advancement in stove design. However, even at decreased total particle concentrations, emissions of compounds that can be harmful for human health can still be high. Examples of such compounds are soot particles and polycyclic aromatic compounds (PAHs), compounds that may cause cancer.

Another frequently used source of combustion aerosols in indoor air is candle burning. Candles should preferably burn with a steady flame. However, in real indoor environments, air movements in the surrounding air caused by human movements and drafts from doors and windows are difficult to avoid and will cause flickering of the flame. Flickering candle flames are known to emit soot particles. This phenomenon can even be observed with the naked eye as a black puff of smoke coming from the candle flame when it flickers. However, the effect of the wax and wick material on emissions of soot and other pollutants is largely unknown. Emissions from the flickering burn of five candle types of similar shape but different wax and wick material were measured to study the influence of candle materials on the pollutant emissions. The results showed strong variations in the soot emissions between candle types. The candles with the lowest soot emissions also showed high emissions of ultrafine particles, which has a high probability of depositing in our lungs upon inhalation. Contrary to soot emissions, the levels of the gaseous pollutants NO_x, formaldehyde, and gas-phase PAHs, which are of concern for human health, varied much less among the tested candles. While reduction in soot emissions can be obtained by an optimized wax and wick combination, NO_x, formaldehyde, and the emission of gas-phase PAHs proved harder to prevent from candle burning.

Concerns have been raised about the widespread use of chemicals in consumer products. Many of these chemicals enter the market without sufficient testing and with little knowledge about their safety. Because of their frequent use, they find their way into our homes via building materials and consumer products. Phthalates are a group of such chemicals that has gained increasing attention over the past decades because some phthalates disrupt the human hormone system. Phthalates are, for instance, ingredients in personal care products (for example, diethyl phthalate [DEP]) and are used as plasticizers to increase the flexibility of plastic materials (for example, di-(2-ethylhexyl phthalate) [DEHP]). Because phthalates are not chemically bound in the material, they can evaporate into the surrounding air. In the thesis research, the uptake of DEHP, emitted from polyvinyl chloride (PVC) flooring, onto different particle types was measured. The results showed increased emissions of DEHP from the PVC flooring in the presence of particles. The results also showed a higher uptake of DEHP in indoor particles with a higher content of organic compounds compared to salt particles produced in the laboratory.

Besides exposure via inhalation, our skin is also exposed to surrounding air pollutants. To evaluate the human uptake of phthalates via skin and inhalation, a human exposure study was conducted. Sixteen voluntary participants were exposed for three hours to either a gas-phase phthalate (DEP) or to a particle phase phthalate (DEHP). They were exposed via both skin and inhalation in a combined exposure, and via skin only, with the participants breathing clean air through a hood. The gas-phase DEP uptake was observed via both inhalation and skin, with the inhalation uptake being approximately ten times higher compared to skin uptake. The participants wore clean clothing and showered after exposure, which may have rendered partial protection against uptake via the skin. No uptake via the skin was measured from particle phase DEHP exposure. The inhalation uptake of DEHP was four times lower compared to DEP, which may reflect the differences in the lung deposition of gases and particles.

These results emphasize the importance of chemical characterization and quantification of indoor particle emissions, and the need to consider the properties of aerosols and chemicals in risk assessments. The content of organic compounds in particles is often high in indoor environments, which may increase the uptake of DEHP on particles, which can end up in the human lung upon inhalation. To keep chemical exposure levels at a minimum, both harmful chemicals in consumer products and particle concentrations should be reduced.

List of Abbreviations

AMS	Aerosol Mass Spectrometry
AER	Air Exchange Rate
BBP	Benzyl Butyl Phthalate
BC	Black Carbon
BTX	Benzene, Toluene, Xylenes
CO	Carbon Monoxide
CPC	Condensation Particle Counter
DBP	Dibutyl Phthalate
DEHP	Di-(2-ethylhexyl) Phthalate
DEHTP	Di-(2-ethylhexyl)-terephthalate
DEP	Diethyl Phthalate
DIBP	Diisobutyl Phthalate
DINCH	1,2-Cyclohexane Dicarboxylic Acid Diisononyl Ester
DMA	Differential Mobility Analyzer
eBC	equivalent Black Carbon
EC	Elemental Carbon
EFs	Emission Factors
FA	Fuel Addition
FDGS	Forced Draft Gasifier Stove
FTIR	Fourier Transform Infrared Spectrometer
EFs	Emission Factors
GC-MS	Gas Chromatography-Mass Spectrometry
HACA	Hydrogen-Abstraction-C_2H_2-Addition
HS	Heating Stoves
IARC	International Agency for Research on Cancer
LC-MS/MS	Liquid Chromatography and Tandem Mass Spectrometry
MPPD	Multiple-Path Particle Dosimetry
NB	Nominal Burn Rate
NDGS	Natural Draft Gasifier Stove

NO_x	Nitrogen Oxides, NO and NO_2
OA	Organic Aerosol
PAH	Polycyclic Aromatic Hydrocarbon
PAM OFR	Potential Aerosol Mass Oxidation Flow Reactor
PM	Particulate Matter
PNC	Particle Number Concentration
POA	Primary Organic Aerosol
PVC	Polyvinyl Chloride
REACH	Registration, Evaluation, Authorization and Restriction of Chemicals
RIE	Relative Ionization Efficiency
RS	Rocket Stove
rBC	Refractory Black Carbon
SMPS	Scanning Mobility Particle Sizer
SOA	Secondary Organic Aerosol
SP-AMS	Soot Particle Aerosol Mass Spectrometer
SVHC	Substance of Very High Concern
SVOCs	Semi-Volatile Organic Compounds
ToF	Time of Flight
TSP	Total Suspended Particulate Matter
UFPs	Ultrafine Particles
VHB	Very High Burn Rate
VOCs	Volatile Organic Compounds
3S	3-Stone Fire

Background

Aerosols are made of liquid or solid particles suspended in a gas. Aerosols are ubiquitous in the atmosphere, and play a central role for human health and climate. Exposure to aerosol particles, more specifically fine particulate matter ($PM_{2.5} < 2.5$ µm), has been associated with a wide range of health effects in humans. Examples are cardiovascular and respiratory diseases,[1] chronic obstructive pulmonary disease, asthma,[2] and allergies.[3] Each year exposure to air pollution leads to an estimated 7 million premature deaths globally, of which 3.8 million are caused by household air pollution.[4] In addition to health effects, air pollution poses environmental and climate challenges. Aerosol particles affect the climate with their direct and indirect radiative forcing,[5] and black carbon has been assessed to be the second largest contributor to global warming after CO_2.[6] The health effects and climate forcing strength depend on the chemical composition and physical properties of aerosols. It is therefore important to study the physicochemical characteristics of aerosols from major sources. The influence of combustion conditions on the detailed chemical composition of aerosols emitted from cookstoves and candles is not well understood, and is of importance for the evaluation of health effects from exposure to combustion aerosols.

Air pollution is disproportionately distributed with approximately 90% of the premature deaths occurring in low- and middle-income countries.[4] Household air pollution from solid fuel combustion in developing countries is associated with severe health effects such as pneumonia, heart disease, and chronic obstructive pulmonary disease. Approximately 3 billion people around the world depend on solid fuel combustion for cooking and heating.[7] Women and children experience the highest exposure to household air pollution. Infants are often kept in near proximity to their mother while cooking, and are thereby exposed to air pollutants when their immune system is still vulnerable.[8]

Chemical pollution is an increasing global problem. Since 1950 more than 140 000 new chemicals has been synthesized. The 5000 chemicals that are produced in the largest quantities are widely distributed in the environment. Many of these have undergone little testing for toxicity and environmental safety before entering the market.[4] These chemicals have contributed to the innovation and development of new materials. However, the increasing use of chemicals is also associated with detrimental effects on human health and the environment. Endocrine disrupting chemicals are one example. The burden of disease for endocrine disrupting chemicals in Europe has been estimated to a yearly cost of 163 billion Euro, which is likely underestimated because it only includes limited health outcomes and chemicals.[9] Semi-volatile organic compounds (SVOCs) make up one group of chemicals that are frequently used in consumer products, for example phthalates. They can migrate from their original material into the air, making up exposure routes for humans in indoor environments. Some SVOCs including phthalates are known to disturb the endocrine system.[10] It is therefore important to gain increased knowledge about the (airborne) exposure to such chemicals. Some phthalates are of concern because of their endocrine disruptive properties in humans,[11] and their ubiquitous distribution particularly in indoor environments. Costs associated with male infertility in Europe due to phthalate exposure have been estimated to be approximately 5 billion Euro annually.[12] Because of their semi-volatile properties, some phthalates will distribute in both the particle- and gas-phase. In the presence of particles, phthalates in the gas-phase can sorb to particles, resulting in a change of phase from gas to particles.[13] In that way, particles can act as carriers of phthalates and other SVOCs and transport them deeper into the lungs where they can translocate to other organs. A thorough investigation of the phthalate sorption to particles is still lacking, and the influence of phthalate particle exposure on humans is not well studied.

This thesis concerns the physicochemical characterization of aerosols from combustion sources; more specifically, from cookstoves, relevant for developing countries, and candles, relevant for both developing and industrialized countries, that significantly contribute to household air pollution. Whereas cookstoves additionally contribute to ambient air pollution and impact both health and climate. The research also examines the human uptake of phthalates through exposure via the skin and via inhalation, as well as the sorption of a specific phthalate onto particles of different chemical composition. Altogether, this includes aerosol emissions from sources, which contribute to household and ambient air pollution, that are of concern due to human exposures and the associated health effects.

Aims and Objectives

The aim of the research presented in this thesis was quantification and physicochemical characterization of the emissions from typical indoor aerosol sources e.g. cookstoves and candles. In this thesis, the sorption of a common phthalate on particles was assessed and the human exposure to phthalates was evaluated. To carry this out, in-situ and highly time-resolved methods were applied. The results contribute to an increased understanding of the role of particles in exposures to human-made chemicals and endocrine disruptors in the indoor environment.

The specific aims were

Paper I: To chemically characterize aerosol emissions from different biomass cookstoves, and to evaluate the influence of the combustion conditions on primary and secondary particle emissions.

Paper II: To physicochemically characterize aerosol emissions from the controlled stressed burning of candles, and to evaluate the emissions' influence on indoor air quality.

Paper III: To assess the sorption of a commonly used semi-volatile phthalate on particles of different chemical composition, and to understand the role of particles as carriers of semi-volatile organic compounds (SVOCs).

Paper IV: To evaluate the human uptake of airborne phthalates in the particle and gas-phase through a human exposure study of dermal and inhalation exposure to two commonly used phthalates.

Introduction

Indoor Aerosols

Our exposure to air pollution primarily occurs indoors as we spend approximately 90% of the time in indoor environments in Europe and in Northern America.[14, 15] It is therefore important to characterize and quantify levels of indoor air pollution including contribution from specific indoor sources, as well as to assess the human exposure indoors.

Concentrations of indoor air pollution are influenced by active indoor sources (e.g. candles and cookstoves) as well as pollutants of outdoor origin infiltrating to indoor air via ventilation, airing practices (window and door openings), and penetration through the building envelope. Thus, ventilation both introduces and removes air pollutants. Concentrations are also affected by the building characteristics, occupant activities (such as candle burning), deposition, coagulation, resuspension, and chemical reactions,[16] which may also result in new particle formation. Deposition constantly changes the levels of indoor air pollution, and is size dependent for particles. It is an important process in indoor environments, where the surface area to volume ratio is high.[17, 18]

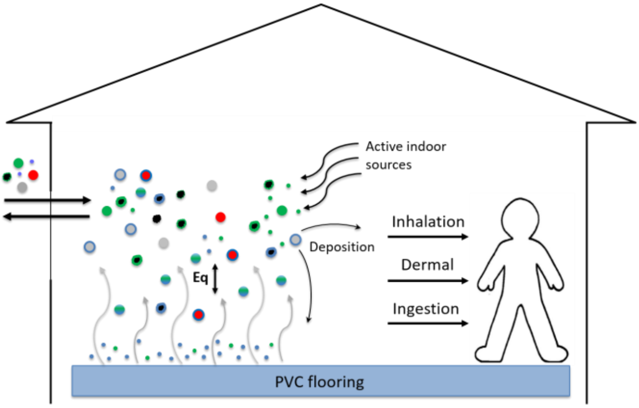

Figure 1 The schematic outlines some of the prccesses influencing the concentrations of indoor air pollution and the human exposure to particles and gases in indoor environments.

The physicochemical characteristics of outdoor particles change upon transport to indoor air, as the penetration efficiency is size-dependent and differences in temperature and humidity between indoors and outdoors can cause volatile components to evaporate from the particles or condensate on the particles.[19]

Particles in indoor air are continuously altered chemically and physically by various processes, one of them being the gas-particle partitioning of semi-volatile compounds (SVOCs).[20] SVOCs are released from consumer products and building materials into indoor air, from where they can *ad*sorb/*ab*sorb to airborne particles, depending on the physicochemical properties of the SVOCs and the particles.[21, 22]

Human exposure to airborne pollutants occurs via inhalation and dermal uptake. Oral exposure can occur via ingestion of e.g. dust containing deposited pollutants,[22, 23] which is not considered in this thesis work. These processes are illustrated in Figure 1, inspired by Thatcher et al.[24]

The chemical composition of indoor air has been found to often have higher concentrations of organic compounds than outdoor air, especially during occupant activities.[23, 25, 26] These organics may include carcinogens such as PAHs, and endocrine disrupting chemicals such as phthalates.[16]

Compound Classes of Relevance for this Thesis

Aerosol particles possess diverse chemical and physical properties. The major chemical components of aerosol particles are well-known. However, the specific chemical composition depends on the emission source, particle size, etc. The diversity in the chemical and physical properties of aerosol particles complicates one’s ability to determine the linkage of exposure to human health effects. This section presents the particulate matter (PM) components that are in focus in this thesis.

Organic aerosol (OA) is a broad term covering thousands of organic chemical compounds in aerosol particles. OA is divided into primary organic aerosol, covering the OA emitted directly into the atmosphere, and secondary organic aerosol (SOA), covering the OA formed chemically from gas-phase precursors in the atmosphere, either from new particle formation or addition of mass to pre-existing particles. OA toxicity largely depends on the particle chemical composition, which is why it is important to study the OA composition.

Black carbon (BC) refers to mature strongly absorbing soot particles.[27] BC is generated under incomplete combustion conditions, described in more detail on page 24. Inhalation exposure to BC particles is associated with morbidity[28, 29] and mortality.[30] The light absorbing properties of BC are of concern for climate due to global warming. The presence of BC in indoor environments has typically been associated with penetration from outdoors. However, it is important to consider possible indoor sources of BC emissions such as cookstoves and candles (Papers I and II).

When BC is measured with light absorbing techniques it is denoted as equivalent BC (eBC). When measured by means of heating through high-power long-wavelength (e.g., 1064nm) lasers, such as in soot particle aerosol mass spectrometry (SP-AMS), the refractory black carbon is measured and referred to as rBC. The measurement technique for BC is as such different from that for elemental carbon (EC), which is refractory carbon measured with thermal optical methods.[31]

Semi-volatile organic compounds (SVOCs) are a class of organic compounds with vapor pressures in the range of 10^{-9} to 10 Pa.[20] SVOCs with intermediate vapor pressures will partition between the gas-phase and particles. Some SVOCs are of health concern.

> **Phthalates** are a group of SVOCs, which are ubiquitous in indoor environments, because of their extensive use in many consumer products. Some phthalates are of concern for human health, because of their endocrine disrupting properties.[32] Phthalates are described in further detail on page 27.
>
> **Polycyclic aromatic hydrocarbons (PAHs)** make up a group of OA components, which are widely studied due to their carcinogenic properties.[33] PAHs are formed in incomplete combustion reactions and are classified as a group 1 carcinogens (carcinogenic to humans) by the International Agency for Research on Cancer (IARC).[34] PAHs are reported as benzo(a)pyrene equivalent (BaP eq) concentrations with the relative importance of the individual PAH compounds for the total cancer risk based on toxic equivalence factors. Their roll in soot formation make them a significant organic component of soot particles. The lower molecular weight PAHs with higher vapor pressures belong to the class of SVOCs.

Inorganic aerosol components such as nitrate, sulfate, and ammonium make up a significant proportion of ambient $PM_{2.5}$ and have also been characterized in this thesis (Paper II).

Major gas-phase compounds including NO_x (NO_2 and NO), carbon monoxide (CO), PAHs, and benzene, toluene, xylenes (BTX) are emitted from combustion sources and are also associated with various health effects due to exposure. Exposure to CO is associated with neurobehavioral and cardiovascular disease and CO poisoning is responsible for unintentional deaths.[35] Exposure to NO_2 causes negative health effects upon inhalation[36], and benzene is classified as carcinogenic[37], while toluene impacts the central nervous system.[38]

Combustion Aerosol Sources

Cookstoves

Approximately 3 billion people around the world depend on solid fuel combustion for cooking and heating.[7] It has long been recognized that the use of cookstoves emits high concentrations of air pollution that are of concern for both human health and climate.[39, 40] Poor air quality is associated with infant mortality in Africa.[41] The traditional cookstoves applied in developing countries are fuelled with solid biomass fuel, such as wood, crops, waste residues, and charcoal. Several newer designs of cookstoves have been marketed and sold as improvements of the traditional cookstoves. And several studies report reduced pollutant emissions of $PM_{2.5}$ and CO emissions from improved stoves,[40, 42-45] as well as reductions in methane and VOC emissions.[46]

The cookstoves studied in Paper I are of Kenyan origin, Figure 2. In Kenya, 92% of the population cook indoors (50% inside the home, 42% in a separate building) and 7% cook outdoors.[47] The traditional cookstove is based on the simple construction of three stones, hence the name 3-stone fire. The 3-stone fire is an open fire in-between three stones. The rocket stove is an improved cookstove fuelled with wood sticks, with its characteristic elbow-shape serving as a combustion chamber, and with added insulation compared to the 3-stone fire.

Some advanced cookstoves rely on gasification, in which the combustion gases are produced from biomass fuel, and the gases are mixed with air, and then combusted. The natural draft gasifier stove (NDGS) is an advanced cookstove technology where the primary air is supplied from the bottom, to create better conditions for volatilization of the energy rich fuel gases for subsequent combustion. The secondary air is introduced above the fuel bed. The purpose of the secondary air supply is to create better mixing of the combustion gases and air. The forced draft gasifier stove (FDGS) is the most technologically advanced cookstove studied in Paper I. It is based on the same principle as the NDGS, but the air supply is driven by an electrically powered fan, ensuring better mixing and reducing air starved fuel rich regions. Both gasifier cookstoves are fuelled with pellets. Figure 2 shows the four cookstoves which are studied and described in Paper I.

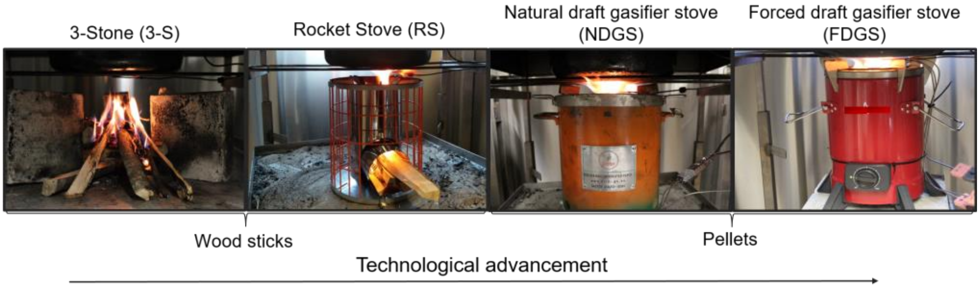

Figure 2 The four cookstoves studied in Paper I. From the left 3-stone fire (3S), rocket stove (RS), natural draft gasifier stove (NDGS), and forced draft gasifier stove (FDGS).

Challenges and Limitations in Adoption of Cleaner Fuels and Stoves

Several intervention programs have been conducted where traditional cookstoves were substituted with improved or advanced cookstoves, some without demonstrating any clear improvements in health benefits[48] or emission reductions.[49, 50] While several laboratory studies have shown decreased $PM_{2.5}$ emissions from improved and advanced cookstoves relative to traditional ones,[40, 42, 44, 51-54] emission reductions in field measurements have shown to be less pronounced than in laboratory studies. This is likely due to operation conditions and fuel properties.[40, 43, 50] Other studies of the health effects have shown health benefits from improved stoves.[55, 56]

Another approach has focused on the use of cleaner fuels and the implementation of technologies that do not rely on solid biomass fuel, rather than implementing improved and advanced biomass cookstoves that do. A number of studies show that the adoption of cleaner fuels like liquefied petroleum gas (LPG), biogas, alcohol fuels, and solar stoves in low- and middle-income countries would result in both health and climate benefits.[57, 58] This implementation has also been suggested to contribute to at least five of the UN sustainable development goals: 3) good health and well-being, 5) Gender equality, 7) affordable and clean energy, 13) climate action, and 15) life on land.[57] LPG in particular has been highlighted as a cleaner alternative to solid biomass fuels.[44, 59]

From the political and regulatory side, the focus has been on promoting renewable biomass (wood and charcoal), as opposed to LPG, which is based on fossil fuel, and therefore assumed to have negative impacts on climate.[8] Thus, there is a trade-off between the possible climate benefits of biomass and the possible health benefits of LPG.[57, 60]

The implementation of cleaner fuels and technologies in the developing world is challenging. Myths and perceptions about cleaner cooking fuels and technologies exists, and limitations in the infrastructure (i.e., fuel supply) hinder the implementation. Examples are that LPG poses a higher risk of explosion, and that food cooked on traditional stoves tastes better. Communication, information, and awareness are tools to overcome these perceptions. Training the population in the use of LPG has shown to be successful, and to reduce the number of explosions in communities unfamiliar with LPG usage. The use of LPG is generally cheaper, but has the disadvantage of having a high one-time payment for the cylinders, which is unattractive for low income households. This contributes to the perception that cleaner fuel is more expensive. Firewood in rural places can often be collected for free, but the collection is often time-consuming and involves drudgery, which most often is not considered as a cost of the fuel.[61]

Attempts to implement clean fuels and technologies have in many cases been marketed based on their health benefits. However, this is not yet a priority for the majority of the population in low- and middle-income countries that rely on traditional stoves and fuel.[62] Thus, according to the WHO, the marketing strategy should rather focus on cost- and time-efficiency and the clean fuels should be promoted during the rainy season when wood fuel is unreliable (moist fuels generate elevated emissions and thereby elevated exposures), and at harvest time when the income in most rural households has increased. Influencers and television should be used to kill the myths about better tasting food cooked with traditional technologies, and promote clean fuel and technologies as female empowerment.[47]

Candles and Their Burning Modes

There is a long tradition of burning candles in indoor environments. Candles previously functioned as an important light source. Nowadays they are primarily burned for decorative purposes and for religious traditions. The burning of candles was first described scientifically in Faraday’s lectures in 1860.[63] When a candle is lit, the wax is liquefied and transported to the flame via the wick by capillary movements. The wax evaporates and enters the reaction zone where it undergoes thermal decomposition.

Many parameters influence the emission of pollutants, one of which is the burning conditions of the candles. A steady burn mode, with no or minor disturbances of the flame, has been associated with increased emissions of inorganic ultrafine particles.[64] A stressed burn mode, introduced by disturbances of the flame caused by surrounding air movements, has been linked to increased emissions of soot particles.[64-66] The smouldering burn of candles, occurring when the candle is extinguished, has been associated with increased emissions of larger-sized particles up to 800 nm with a high content of organic compounds.[65]

Sustainability Aspects of Candles

Candles can be produced from a variety of wax and wick materials. Paraffin and stearin wax are common candle wax materials. Paraffin has its origin in fossil fuels, while stearin wax traditionally is an animal based by-product. Stearin wax is traditionally animal based, but it can also be produced from vegetable oil such as palm oil. Traditional stearin wax is considered renewable because of its origin as a by-product. To obtain the Scandinavian ecolabel (the "Swan" label), the majority of the wax material is required to be renewable, and the use of soy and palm oil is banned.[67]

Palm oil has become a universal ingredient in everyday products, and the demand is projected to increase partly because of its high yield and low production cost.[68] The production of palm oil is tied to deforestation, often of rainforest. This has the consequences of increasing greenhouse gas emissions, reduction in biodiversity, and habitat fragmentation.[69]

PAH and Soot Formation

The soot formation in a diffusion flame, for example a candle flame, starts with the formation of gas-phase soot precursors from incomplete combustion. Formation of the first aromatic ring structure, often benzene or phenyl radicals, is followed by subsequent PAH growth.[70] The HACA (hydrogen-abstraction-C_2H_2-addition) is the most well-known PAH growth mechanism. By hydrogen abstraction, a radical is formed where the addition of C_2H_2 can occur, resulting in PAH growth.[71] However, this is just one of many mechanisms for PAH growth, which may depend on the molecular structure of the fuel as well as the conditions in the flame.[70]

This is followed by particle nucleation, and this step from gas to condensed phase is referred to as soot inception.[27] Different soot nucleation pathways have been suggested, one involves fullerene structures. The soot particles that have evolved beyond inception and not fully carbonized yet are referred to as "partially matured soot" in this thesis.[27]

Next comes the surface growth by gas molecules sorbing to the soot surface. The primary particles formed can then either undergo coalescence (liquid primary particles merging to form a new spherical particle) and/or agglomeration (point contact between primary particles) to form solid aggregates of primary particles. At perfect burn conditions, all the soot particles formed are removed by oxidation in the flame[70, 72] (Figure 3).

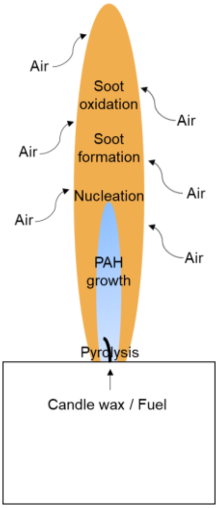

Figure 3 Schematic of an unperturbed candle flame showing the pyrolysis, PAH growth, nucleation, soot formation, and soot oxidation upwards the flame.

If the flame is influenced by surrounding air movement, the temperature drops and reduces the oxidation processes. Soot volume fractions are highest at the mid-height of the flame. Further upwards in the flame, soot oxidation processes become more dominant, and soot oxidation is at its maximum at the top of the flame.[73] OH radicals and molecular oxygen play important roles in the soot oxidation. Thus, soot emissions are governed by two opposing mechanisms, namely, soot formation and soot oxidation.[70, 72, 74] There are still many knowledge gaps in the detailed understanding of soot formation, but the general steps outlined above seem to be generally acknowledged. Nitrogen oxides (NO_x) are formed at the outer edge of the flame where there is a surplus of oxygen, high temperature, and N_2 from the surrounding air.[75]

Pyrolysis and Combustion of Lignocellulosic Biomass

Lignocellulosic biomass, such as wood and crops, consists of the three main components: cellulose, hemicellulose, and lignin. Other trace compounds are water, inorganic compounds, as well as a number of other organic compounds.[76] Cellulose is the main constituent of most lignocellulosic biomass, followed by lignin, and hemicellulose with an approximate distribution in softwood of 42%, 28%, and 27 %, respectively.[77]

The processes in biomass thermochemical conversion include evaporation of water, pyrolysis including volatilization of solid biomass, flaming combustion of the released gases, and smouldering combustion. Pyrolysis (thermal degradation in the absence of O_2) of cellulose occurs via decomposition leading to the formation of the anhydrous sugar levoglucosan and its molecular isomers. Because of its ability to decompose to low-molecular weight volatiles and to form polymer anhydrous compounds, it is as such not the only emitted product from cellulose/biomass pyrolysis.[76] Levoglucosan has been used as a marker for biomass combustion in atmospheric studies.[78] Lignin is a polymer containing aromatic ring-structures, and the pyrolysis of lignin primarily leads to the formation of phenolic compounds, including methoxyphenols. Hemicellulose breaks down to low-molecular heterocyclic compounds such as furfural and 3-4 carbon containing fragments, such as alcohols and carboxylic acids, when pyrolyzed.[79]

Hemicellulose undergoes decomposition at lower temperatures than cellulose, which in turn decomposes at lower temperatures than lignin. It is during the pyrolysis of biomass combustion that the majority of the volatile organic compounds are emitted, while CO_2 and NO_x primarily are formed and emitted from flaming combustion.[80]

The organic compounds that are volatilized under pyrolysis conditions, and are liquid under ambient conditions are termed tars. Tars are divided into primary, secondary, and tertiary tars. Primary tars include sugars such as levoglucosan, phenolic compounds such as methoxyphenols, and heterocyclic compounds. The secondary tars generated at increasing temperatures are primarily from chemical reactions of the primary phenolic compounds generated from lignin. The secondary tars may keep their phenol functionality (other functional groups can have changed) and include phenol and phenol derivatives. Secondary tars also include compounds that have undergone further thermochemical conversion, where the functional groups containing oxygen are lost, such as the aromatic compounds benzene, toluene, and xylenes (BTX). Tertiary tars are generated at further increased temperatures and include PAHs. They are primarily from the phenolic compounds generated from lignin, but can also be generated in lower yields from cellulose.[81-83] In the simplified thermochemical conversion framework presented in Paper I and in Figure 10, the emission class primary pyrolysis products includes the primary tars , and the emission class converted pyrolysis products is comprising the secondary tars and tertiary tars.

The soot formation in the combustion of lignocellulosic biomass in the cookstoves described above is assumed to rely on principles that are similar to the ones described for candles, page 24. However, the combustion in cookstoves is more complex due to turbulence and the non-uniform conditions in the combustion chamber. The latter may also result in volatiles escaping around the flame.[84] A further difference is the fuel and its content of aromatic compounds, as described above, relative to hydrocarbon fuels. Thus, aromatic compounds are available for PAH formation and growth. Fuel moisture has previously been found to increase $PM_{2.5}$, CO, and benzene emissions[85, 86] Increased insulation (e.g. in rocket stoves) has been found to reduce CO and $PM_{2.5}$ emissions, but on the other hand increase emissions of PAH precursors and EC.[44]

Phthalates in Indoor Environments

Phthalates are a group of SVOCs that are used in a wide range of consumer products. Two commonly used phthalates include diethyl phthalate (DEP) and di-(2-ethylhexyl) phthalate (DEHP). DEP is commonly used in personal care products, such as cosmetics, deodorants, fragrances, creams, and lotions. DEHP is a colorless, viscous, and lipophilic liquid, and is mainly used as a plasticizer in medical devices and in a wide range of consumer products, including polyvinyl chloride (PVC) products.[87] Humans are exposed to phthalates via inhalation, dermal absorption, and ingestion,[23, 88] with airborne exposure occurring via inhalation and dermal absorption. Because of the widespread application of phthalates and their omnipresence, people are exposed to phthalates on a daily basis worldwide.[89-91] The airborne exposure pathways depend on the physicochemical characteristics of the individual phthalates and their concentration in different microenvironments.[23] However, the human exposure to airborne phthalates is not well understood.

The associated health effects caused by human exposure to DEHP are primarily endocrine disruption causing reproductive effects.[12, 92-97] However, a wide range of other health effects has been associated with exposure to DEHP, such as allergies,[32, 98-100] cardiovascular disease, neurocognitive effects,[101, 102] and obesity.[97] Prenatal exposure and child exposure are of particular concern and may cause more severe effects than adult exposure.[96, 103-106]

DEHP, which was studied in Papers III and IV, is now classified as a substance of very high concern (SVHC) under REACH (registration, evaluation, authorization and restriction of chemicals) (REACH, Annex XVII). The restricted use of DEHP in Europe has been revised continuously, with the latest restriction coming into force in July 2020 regarding the use of DEHP and three other phthalates: BBP, DBP, and DIBP. According to REACH Annex XVII, it is no longer allowed to market articles with a mass percent higher than 0.1% of any of the four phthalates, individually or in combination. An additional approach to limiting the use of endocrine disrupting substances has been introduced by REACH as the New Chemicals Strategy for Sustainability. The strategy specifies that “endocrine disrupting chemicals will be banned from consumer products as soon as they are identified”, and that only essential use for society is allowed. However, the required degree of scientific evidence of harmful effects for “as soon as they are identified” is not specified, which is most likely important for the effect and influence of the new strategy.

The use of chemicals is also included in the UN Sustainability Goals as part of the 12th goal: Responsible Consumption and Production.

Before the restricted use of DEHP went into effect, DEHP was a main constituent in PVC floorings with a content of 10-60 % by mass.[13] Previous studies have established that DEHP from PVC flooring will be emitted continuously for decades.[107,108] Since DEHP is not covalently bound in consumer products, it can migrate to the surface of the material and form a so-called surface film, from where it can evaporate.[109] In indoor environments it will distribute in the gas-phase and in particles, on settled dust, and deposit on indoor surfaces. This suggests that the restricted use will not effectively have an influence on buildings furnished with PVC floorings and other building materials before the restrictions went into effect. Another challenge is that DEHP-containing consumer products may be imported from areas with no restricted use of DEHP. Thus, DEHP and other phthalates are still measured in dust in European indoor environments.[110]

After the implementation of restricted use of DEHP in the European Union, it has been replaced by other alternatives. Examples of DEHP substitutes are di-(2-ethylhexyl)-terephthalate (DEHTP), and a compound manufactured under the name DINCH (1,2-Cyclohexane dicarboxylic acid diisononyl ester). A decrease in urinary DEHP metabolites and an increase in DEHTP and DINCH urinary metabolites have been observed in Europe and the U.S.[90, 111, 112] Like DEHP, DEHTP and DINCH are diesters with C8 carbon chains, DEHTP is like DEHP with the side chains placed in para position and DINCH with a heterocyclic ring instead of an aromatic ring. The physicochemical properties are therefore in many ways similar to those of DEHP. The toxicological effects of DEHTP and DINCH are still being evaluated. Thus, unfortunately, it is likely that the presence of phthalates and phthalate-like compounds in our surroundings will continue and it is important to understand the exposure routes.

Gas-Particle Partitioning

Aerosol particles in indoor environments alter over time. One process, which contributes to the alteration is the partitioning of chemicals, namely SVOCs, between the gas-phase and particles. Parameters that can influence the gas-particle partitioning are the compound’s characteristics, its polarity, hygroscopicity, and reactivity, along with environmental factors such as temperature and humidity. The *ad*sorption onto particles and *ab*sorption of chemicals into particles depends on their vapor pressure, but also on the chemical composition of the aerosol particles.[21, 113]

Organic aerosols tend to account for a high mass fraction of $PM_{2.5}$ in indoor aerosol particles.[23, 25] Therefore, absorption may be an important mechanism in indoor air.

The distribution of SVOCs between the gas-phase and the particle phase is a strong function of the vapor pressure. The vapor pressure of DEHP is 1.9×10^{-5} Pa and that of DEP is 1.5×10^{-2} Pa.[114] By using these vapor pressures, which may be in the higher end, the gas-phase is saturated at maximum 3 µg m^{-3} for DEHP and at 1350 µg m^{-3} for DEP. Benning et al. showed experimentally that DEHP is emitted from PVC flooring and adsorbed to ammonium sulfate particles, the model particles for infiltrated ambient secondary aerosol. They also showed that the presence of particles increases the emission rate of DEHP from PVC flooring.[13]

The gas-particle partitioning coefficient $K_{gas\text{-}particle}$ (m^3 μg^{-1}) of a compound can be expressed as:

$$K_{gas-particle} = \frac{C}{TSP \cdot y_{0p}} \qquad (1)$$

Where C (µg m^{-3}) is the particle phase concentration of the SVOC, y_{0p} (µg m^{-3}) is the gas-phase concentration of the SVOC, and TSP (µg m^{-3}) is the total suspended particulate matter concentration.[115] The $K_{gas\text{-}particle}$ does not differentiate between the mechanisms of the gas-particle partitioning: adsorption, absorption, or a combination of both.

Respiratory Deposition of Particles and Gas-Molecules

Human exposure to airborne SVOCs is complicated by their existence in both the particle- and gas-phase simultaneously. Exposure to the gas-phase and particle phase pollutants occurs via inhalation, and dermal exposure occurs via air to skin transfer.

Respiratory Deposition of Particles

Airborne particles can deposit in the airways when inhaled. The toxicity of the inhaled particles depends on their chemical composition and the effect depends on where in the airways the particles deposit, which in turn depends on the particle properties size, shape, density, as well as on the breathing pattern.[116] The respiratory system is usually divided into the extrathoracic region (the head airways), the tracheobronchial region (lung airways), and the alveolar region.

Coarse particles deposit by impaction in the extrathoracic region. Ultrafine particles (less than 100 nm) can also have a high deposition fraction in this region due to high diffusivity. The overall deposition in the tracheobronchial region is low. For particles larger than 0.5 µm, the dominant mechanisms are settling and impaction. Ultrafine particles deposit by Brownian motion/diffusion. In the alveolar region, large particles generally deposit by settling and small particles by diffusion. It is in the alveolar region that the gas-exchange occurs.

If the deposited particles are readily soluble in the lung tissue, the particle components enter the blood stream. Surfaces in the extrathoracic and the tracheobronchial regions are covered with a layer of mucus. The insoluble deposited particles are removed by mechanical clearance, when the layer of mucus is propelled upwards and swallowed to the gastrointestinal tract or coughed up. This happens on the timescale of hours. In the alveolar region, soluble material (such as DEHP) can pass through the alveolar membrane and translocate to other organs. Insoluble particles can be engulfed by macrophages and transported to the lymph nodes. However, it can take months to years to clear them. The extrathoracic and the tracheobronchial regions can be considered as protecting the more vulnerable alveolar region from particle deposition.[116]

The particles in the size range of 0.3-0.6 µm show the lowest deposition, and a large fraction is exhaled, because none of the deposition mechanisms – diffusion/Brownian motion, settling, impaction, and interception – are efficient in this size range.[17]

Respiratory Deposition of Gas Molecules

Inhaled gas molecules deposit onto the lung and airway surfaces by diffusion.[117] The uptake of gas molecules in the airways is dependent on their solubility in the lung tissue.[118] A concentration gradient is needed for the transport of gas molecules from the airways to the airway wall to take place by diffusion. The probability of adhering to the airway walls increases with molecule size, because of the larger thermal velocity and the smaller surface of the smaller molecules. The possibility of the molecule dissolving at the surface tissue of the airway wall will lead to a zero concentration at the wall and thereby maintain the concentration gradient. By inhalation of high concentrations, the surface of the airways may saturate, which slows down diffusion. This can result in saturation of the upper airways during exposure, which can lead to deposition deeper down in the lung. The uptake in the airway tissue is thereby proportional to the concentration of gas molecules entering the airways. The gas absorption in the airways depends on the diffusion coefficient and the solubility in the tissue. The more hydrophilic gases will dissolve in the extrathoracic region and are less likely to reach the alveoli; examples are SO_2 and N_2O. For the less soluble gases, it is possible that part of the inhaled concentration will be exhaled.[117]

Deposition of SVOCs on the Skin

The human skin consists of the stratum corneum covered with skin lipids. The stratum corneum consists of several lipid layers. Below this is the viable epidermis and underneath lays the dermal capillaries. Between the bulk air and the skin surface is the boundary layer, which controls the transport of gases and airborne particles to the skin.[119]

Particle Deposition

The size-dependent particle deposition will be affected by Brownian motion (for particles smaller than 0.5 µm), gravitational settling (larger than 1 µm), thermophoresis (the temperature difference between the room air and the skin surface temperature), and electrostatic forces. Furthermore, the airflow turbulence, the orientation of the surface (mainly affecting larger particles where gravitational settling is an important deposition mechanism), and the surface roughness of the skin will influence the deposition velocities.[17]

In Paper IV, gravitational settling and electrostatic forces can be neglected to affect the deposition due to the size distribution and the generation of particles by evaporation-condensation, which most likely only generates a small fraction of charged particles. Thermophoresis can be considered to have a protective effect towards particle deposition on skin surfaces, as particles tend to move towards colder temperatures, with less thermal movement of the surrounding gas molecules.

The transport of particles through the boundary layer, in close proximity to the skin surface, controls the deposition of particles on the skin surface layer. Shi et al. used the following simplified expression to describe the particle deposition of SVOCs onto the skin.[120]

$$J_p = C_p \cdot v_d \tag{2}$$

Here J_p is the mass flux of the particle phase DEHP from the air to the skin (ng m^{-2} h^{-1}), C_p is the particle phase DEHP concentration (ng m^{-3}), and v_d is the particle deposition velocity onto human body surfaces (m h^{-1}). Lai et al. reported deposition velocities of ~ 0.07 m h^{-1} for 100 nm particles on indoor surfaces. [17] For the gas-phase DEP, v_d has been estimated to 5-10 m h^{-1}.[119]

Gas Deposition

For the dermal uptake of gas-phase SVOCs via air to skin transfer, the SVOCs will transport from the gas-phase to the boundary layer of the skin and into the skin lipids, through the viable epidermis, into the capillaries and enter the blood stream. The transfer from the gas-phase to the boundary layer can be described by a mass transfer coefficient.[119] The amount of the deposited mass that enters the blood depends on the transdermal permeability coefficient from air to blood, $K_{p\text{-}g}$, which can be expressed by the gas-phase concentration C_g in the air, and the mass flux to the blood, J_g.

$$J_g = C_g \cdot K_{p-g} \tag{3}$$

$K_{p\text{-}g}$, for the compounds studied in Paper IV has been estimated to be 3.4 m h^{-1} for DEP and 5.8 m h^{-1} for DEHP.[119]

The equation above only applies for the gas-phase. In the human exposure study described in Paper IV, approximately 1 µg m^{-3} of DEHP was in the gas-phase and approximately 100 µg m^{-3} was in the particle phase.

Comparing Deposition of Gas-phase DEP and Particle Phase DEHP

If it is assumed that the DEHP adsorbed to particles behaves in the same way as the DEHP deposited from the gas-phase after deposition on the skin surface, $K_{p\text{-}b}$ is the transdermal permeability coefficient from the skin surface to the blood, which is 140 m h^{-1} for DEHP and 7.9 m h^{-1} for DEP.[119] The limiting factor then becomes the deposition rate, which is around two orders of magnitude larger for gas-phase DEP than particle phase DEHP (5-10 m h^{-1} compared to 0.07 m h^{-1}).

These estimations do not include the barrier provided by clothing. It was estimated by Cao et al. that it is harder for DEHP to permeate clothing than for DEP because the diffusion coefficient of DEHP in clothing is much smaller than that of DEP.[121]

Methods

In Paper I, the health and climate relevant emissions from four cookstoves were chemically characterized with the application of aerosol mass spectrometry (AMS). The cookstoves had distinct design properties, which varied the combustion conditions between the stoves, ranging from a traditional open fire, to a gasifier cookstove with an optimized air supply. The secondary organic aerosol formation was investigated using a potential aerosol mass (PAM) oxidation flow reactor (OFR).

In Paper II, the influence of the wax and wick composition on the aerosol emissions from stressed burning of 5 pillar candles with identical dimensions and shape was investigated in an environmental chamber in order to simulate indoor conditions. The stressed burn was controlled and repeatable. The primary instruments were AMS, a scanning mobility particle sizer (SMPS), and an aethalometer. Additionally, offline sampling was performed for subsequent analysis of PAHs and thermo optical analysis.

In Paper III, the influence of the particle chemical composition, residence time, and particle concentration on the sorption of di-(2-ethylhexyl) phthalate (DEHP) on particles was investigated with the application of AMS measurements. The study was conducted in a 1.2 l aluminium chamber equipped with PVC flooring containing DEHP.

In Paper IV, the dermal and inhalation uptakes of two airborne deuterium-labeled phthalates, one gas-phase and one particle phase phthalate, were examined in a human exposure study with 16 volunteers. Four participants at a time were exposed for three hours in a human exposure chamber while wearing clean clothing, with a subsequent collection of urine samples. The airborne concentrations were measured *in situ* with AMS and SMPS, and via offline sampling for subsequent analysis with gas chromatography - mass spectrometry (GC-MS). Metabolites were measured in the urine samples for the evaluation of human uptake.

Measurements of Cookstove Emissions (Paper I)

Emissions from four different cookstoves were measured: 1) a traditional 3-stone fire (an open fire), 2) an improved elbow-shaped rocket stove with added insulation to the combustion chamber, 3) an advanced natural draft gasifier stove (NDGS), and 4) an advanced forced draft gasifier stove (FDGS), where the primary and secondary air supply was controlled by an electrical fan (Figure 2). The 3-stone fire and the rocket stove were fueled with casuarina wood sticks collected in Kenya. The NDGS and FDGS were fueled with three different pellet fuel mixtures identical for each stove: 1) pure Nordic softwood standardized pellets of pine and spruce, 2) Nordic standardized pellets in mixed 50:50 with bagasse, and 3) Nordic standardized pellets mixed 50:50 with coffee husk. The instrumental setup used for measurements of fresh and aged cookstove emissions in Paper I is shown in Figure 4.

The cookstoves were lit with ethanol, and a pot of water with a lid was placed above the stove. An extraction hood was used for sampling and dilution of the emissions, with further dilution by ejector dilutors, described in more detail in Paper I. A modified version of the standard water boiling test was applied. The water boiling test has been developed for testing stove energy efficiency, and consists of a cold start, a hot start, and simmering. In Paper I, studying the emissions from simulated real-life applications of the cookstoves was of interest, so the hot start was excluded from the test.

The online instruments applied for transient measurements were: an SP-AMS measuring aerosol particle chemical composition; a Fourier Transform infrared (FTIR) spectrometer for benzene, toluene, xylenes, and carbon monoxide (CO); an aethalometer for measurement of eBC; and a CO_2 monitor.

For selected experiments, the emissions from the 3-stone fire, rocket stove, and NDGS were transferred to a 15 m^3 stainless steel chamber. The potential aerosol mass (PAM) oxidation flow reactor (PAM OFR) was coupled to the chamber and applied for the measurements of aged emissions to derive the secondary organic aerosol formation (Figure 4). The PAM OFR OH exposure was calibrated with SO_2, described in detail in the supporting information in Paper I. The SP-AMS and aethalometer were measuring after the PAM OFR.

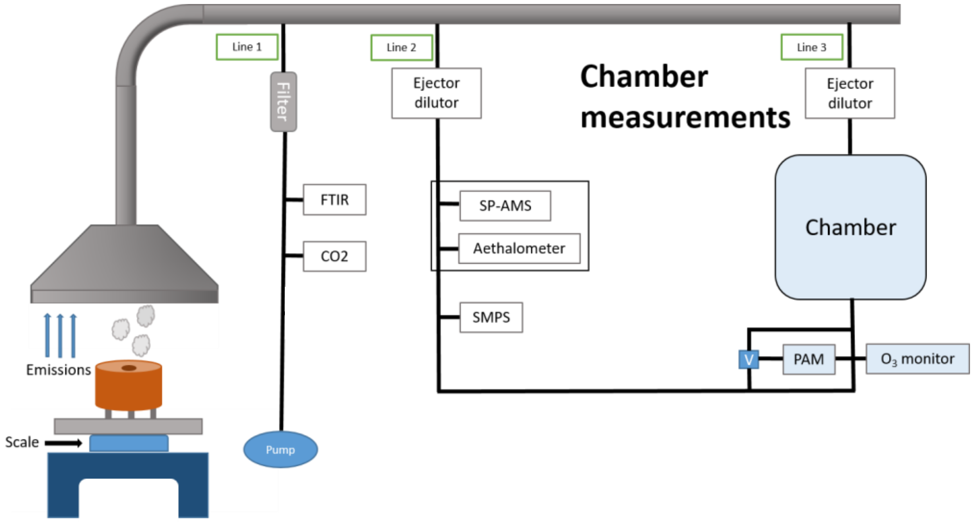

Figure 4 Overview of the laboratory setup applied for measurements of cookstove aerosol emissions in Paper I.

Stressed Burning of Candles (Paper II)

Candles were burned in a 21.6 m^3 stainless steel chamber[122] under controlled stressed burning conditions created with fluctuating air flows generated by a turning electrical fan. The well-mixed aerosol emissions from five candle types of equal shape and size, with different wax and wick material, were measured (Table 1) to study the influence of these materials on the emissions from stressed burning of candles. The wicks of these candles are impregnated, primarily with phosphate, nitrate, sodium, sulfate, and ammonium, in different combinations[123] to protect them from the molded wax and to control the flame height and thereby ensure adequate trimming of the wick. All candles were white and non-scented.

Table 1 Overview of the five candles' materials. The wicks are denoted with a number. The same wick type was applied in candles 1 and 4.[123]

Candle #	Wax material information		Wick #
Candle 1	Animal stearin	Pressed	1
Candle 2	Paraffin (75%) stearin (25%)	Pressed, fully refined paraffin	2
Candle 3	Paraffin	Molded, fully refined paraffin, rustic look	3
Candle 4	Palm stearin	Pressed	1
Candle 5	Paraffin	Pressed, fully refined paraffin	5

Three candles of one type were burned at a time for 3.5 hours with an air exchange rate of 2 h^{-1}. The candles were placed in a triangular geometry with 10 cm distance between each of the candle edges. The fan was placed at a distance of 160 cm from the candles with the neutral position at an angle of approximately 130 degrees. The online sampling was performed with a seven wavelength aethalometer, SP-AMS, SMPS, and a NO_x monitor.

Measurements directly above the flame of each of the five candle types were performed to increase the mechanistic understanding of the processes governing particle emissions. One candle was burned at a time under stressed burn conditions. Measurements of the extinguish smoke (smouldering of the wick) were also performed. To avoid disturbing the flame, the sampling tube was placed approximately 4 cm above the flame and shifted approximately 1 cm to the side. These measurements were performed with AMS, an aethalometer, and a NO_x monitor.

Sorption of DEHP on Particles (Paper III)

Particles were sampled through an aluminium chamber with a volume of 1.2 L and dimensions of 0.45 m×0.25 m×0.019 m (Figure 5).[124] Ammonium sulfate particles, generated with a nebulizer, and indoor aerosols mainly of outdoor origin from the laboratory air were sampled through the aluminium chamber. The half circular chamber was equipped with two sheets of PVC flooring with a mass percent of 13% DEHP. The aerosol particles entered the chamber via the two inlets and were sampled through the mid-outlet (Figure 5). The particles were sampled with AMS, to measure the chemical composition of the aerosol particles passing through the chamber and bypassing the chamber. Additionally, to study the effect of volatile components (primarily organic aerosol compounds) covering the surface of the particles, a thermodenuder (Aerodyne) was applied to remove impurities that were on the ammonium sulfate particles, and to remove volatile components from indoor particles. The setup is described in detail in Paper III.

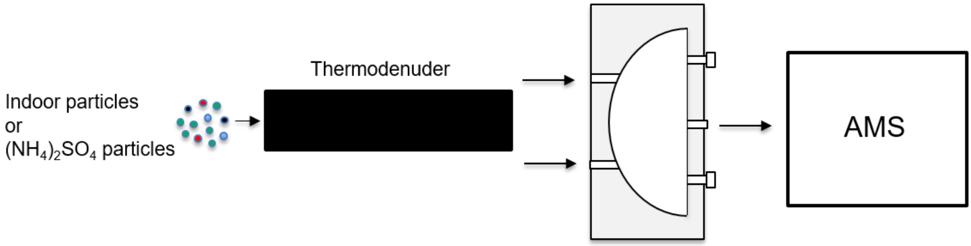

Figure 5 Simplified schematic of the 1.2 L aluminum chamber equipped with DEHP containing PVC Floor.

Study Design of the Human Exposures to Phthalates (Paper IV)

A human exposure study of the dermal and inhalation uptake from exposure to airborne phthalates was conducted. Sixteen participants were recruited to the exposure study of deuterium-labeled diethyl phthalate (D_4-DEP) in the gas-phase, and deuterium-labeled di-(2-ethylhexyl) phthalate (D_4-DEHP) in the particle phase. Deuterium-labeled phthalates, namely D_4-DEP and D_4-DEHP, were used for the exposures to distinguish from the phthalate background contamination. Throughout the text they are denoted DEP and DEHP. The participants were exposed in four exposure scenarios for three hours wearing clean cotton clothing: 1) combined inhalation and dermal exposure to DEHP ($\text{DEHP}_{\text{inh+dermal}}$), 2) dermal exposure to DEHP ($\text{DEHP}_{\text{dermal}}$), 3) combined inhalation and dermal exposure to DEP ($\text{DEP}_{\text{inh+dermal}}$), and 4) dermal exposure to DEP ($\text{DEP}_{\text{dermal}}$). During exposure scenarios 2 and 4, inhalation of the two phthalates was eliminated by having the participants breathe air that was free from deuterium-labeled phthalates through a hood that was sealed around the neck.[125] In these two exposure scenarios, only the dermal uptake from airborne phthalates by air-to-skin transfer, with clean clothing acting as a barrier, was considered. Dermal uptake from phthalates deposited on clothing prior to exposure was out of the scope for this study. The participants showered right before exposure and after the exposure ended, with phthalate free soap. Urine samples were collected before exposure and at regular intervals until 24 hours after exposure. The metabolites of D_4-DEP and D_4-DEHP were analyzed in the urine samples by liquid chromatography, tandem mass spectrometry (LC-MS/MS), described in greater detail in Paper IV.

The particle concentrations during the exposures were measured by an AMS, SMPS (scanning mobility particle sizer), and by the offline collection of particles on Teflon filters connected to sorbent Tenax tubes. The gas-phase concentrations were sampled on sorbent Tenax tubes. Further details are provided in Paper IV. Figure 6 presents a schematic of the study design outlining the exposure scenarios and the stainless steel exposure chamber.

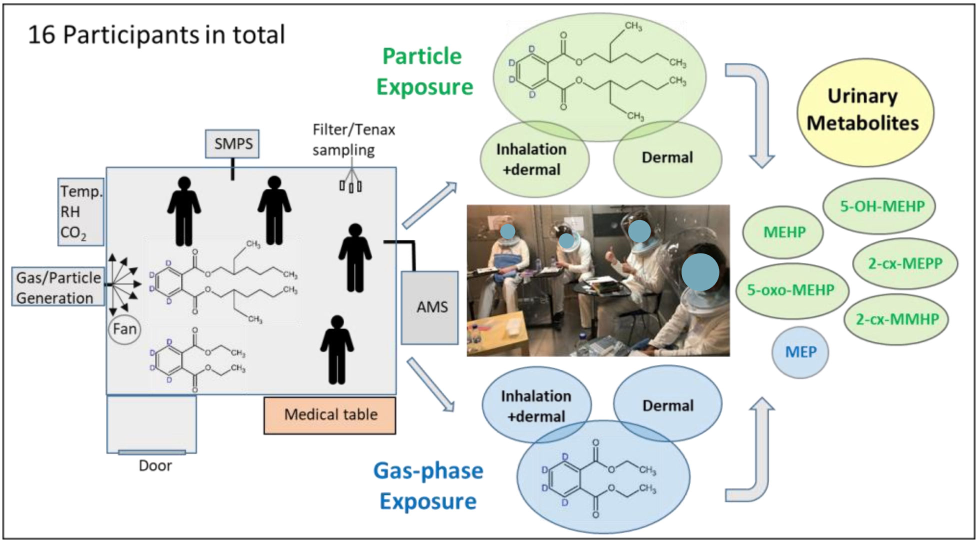

Figure 6 Schematic of the study design and exposure scenarios of Paper IV. Four persons were exposed in each exposure scenario for three hours. Urine samples were collected after the exposure, and were analyzed for metabolites to assess the uptake of DEP and DEHP.

Generation of DEHP Particles

The generation of DEHP particles was achieved by using a prototype of a particle generator developed in-house.[126] The particle generator relies on a heating and condensation principle. An air flow was passed above a small container filled with liquid D_4-DEHP, which was heated. The evaporated vapor was transferred with the airflow into a condensation chamber, where the supersaturated vapor had time to nucleate followed by condensational growth. A second air flow transferred the grown DEHP particles from the condensation chamber into the exposure chamber. To obtain the desired exposure concentrations, several initial tests were performed, including optimization of the holder for DEHP, temperature, and the two flow settings in order to obtain a steady generation of DEHP particles.

Aerosol Mass Spectrometry (AMS)

Aerosol mass spectrometry[127] (AMS) was applied for *in-situ* measurements of aerosol particles in the studies presented in Papers I, II, III and IV. AMS is a technique developed for time-resolved (up to 10 Hz) chemical characterization and sizing of aerosol particles from 50 nm to 1000 nm (PM_1). AMS measures the non-refractory aerosol particle components, which vaporize at 600°C and are ionized by electron ionization. Thus, most organics as well as some inorganics, including most nitrate and sulfate salts, can be detected.

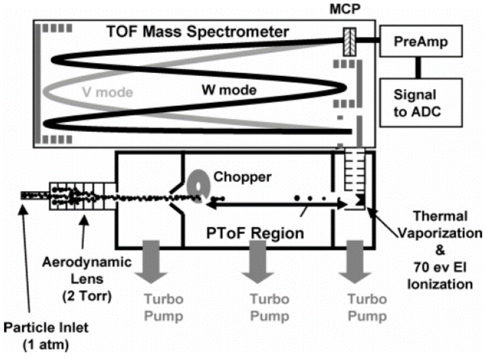

Figure 7 Schematic of an aerosol mass spectrometer (AMS).[127]

Figure 7 shows a schematic of an AMS.[127] It consists of an inlet, a sizing region (particle time-of-flight [PToF]), and a time-of-flight mass spectrometer. Aerosol particles are sampled through an aerodynamic lens and focused into a narrow beam. The aerosol particles impact on a 600°C tungsten plate, under high vacuum conditions generated by several turbopumps, to avoid interference from gas molecules. A chopper is used to measure the instrument background by blocking the particle beam, and to facilitate the particle time-of-flight measurements (sizing region) by modulating the particle beam. Non-refractory material is vaporized, followed by 70 eV electron ionization, and the ions are detected with a high resolution time-of-flight mass spectrometer,[128] with an approximate resolution of 2000 at m/z 200 (nominal m/z/full width at half height).[127]

The soot particle AMS (SP-AMS) is equipped with a laser vaporizer (not shown in Figure 7) for detection of refractory particle components, for example refractory black carbon (rBC), metals, and refractory inorganics. The particles containing refractory material are focused into the laser beam. In the laser beam, the absorbing particle material is heated, and the non-refractory particle components first evaporate. The absorbing refractory material is heated further to sublimation.[129] The evaporated material is ionized by electron ionization as described above.

Quantitative Measurements with AMS – Calibration

In the AMS, a species is quantified by the following equation:

$$C_s = \frac{\sum_i I_{s,i}}{RIE_s \cdot mIE_{NO_3} \cdot Q \cdot CE} \tag{4}$$

where C_s is the mass concentration of a species (µg m^{-3}), RIE_s is the relative ionization efficiency of a species, mIE_{NO3} is the mass specific ionization efficiency of nitrate (ions per picogram of detected particle mass), Q is the flow rate into the AMS (cm^3 s^{-1}), CE is the collection efficiency of the species, and I is the ion count (ions detected per second) summed over all fragments of the species.[129] The relative ionization efficiency (RIE) of a compound is defined as the mIE of a compound relative to the mIE of NO_3, summed over the nitrate signal, primarily at m/z 30 and m/z 46. mIE expresses the number of ions detected per particle mass. It is compound specific, and necessary for quantitative measurements.[128, 129] The collection efficiency of the tungsten vaporizer mode is commonly governed by loss due to bounce off at the vaporizer, for instance, of ammonium sulfate particles. The laser vaporizer is also governed by the loss of detected particles resulting from particles that miss the laser beam. A third collection efficiency term is the loss of detected particles caused by the inlet.[129] The collection efficiency is generally high (~100%) for liquid organic particles and solid particles with a thick organic coating, but significantly reduced (~25%) for solid ammonium sulfate particles.[130]

Ammonium nitrate (NH_4NO_3) particles, size selected to a mobility diameter of 300 nm, are used as a reference to calibrate the AMS. Particles were size selected with a differential mobility analyzer (DMA) and measured with a CPC (number concentration) and the AMS (ions per second). The mass of the particles was calculated by the density of the particle material and assuming spherical particles. For nitrate, a factor of 0.8 was applied to account for pores in the dry particles. Applying this procedure to both ammonium nitrate particles, and to the compound of interest, the RIE of the compound can be determined, shown in Figure 8.

Furthermore, the airbeam (N_2 at m/z 28 signal) is measured and applied to adjust for potential losses or increases in signal intensity over time. When the data is processed, an m/z calibration is applied to all data. It is often based on neighboring peaks with little interference, such as C^+, O^+, O_2^+, Ar^+ and $^{184}W^+$, which are used to make a fit to obtain the position of the peak center.[127, 128] Size calibration of the AMS is performed by comparing the particle diameter and the particle time-of-flight of size-selected monodisperse ammonium nitrate particles or polystyrene latex particles.[131]

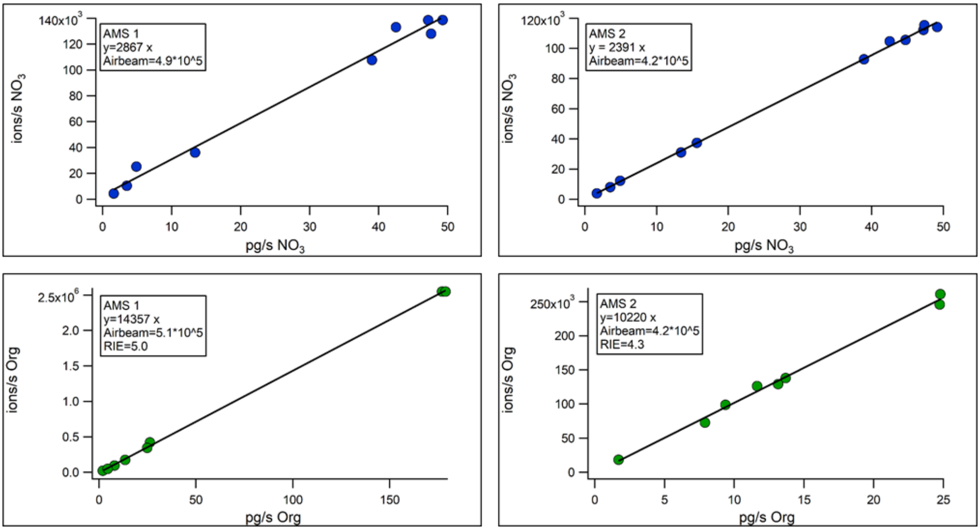

Figure 8 Calibration curves of NO_3 and DEHP of two AMSs showing the ions/s (AMS) plotted against pg/s (CPC). The mass ionization efficiency (mIE) for each compound is derived from the slope of the graphs.

The electron ionization applied in AMS leads to strong fragmentation of a majority of the evaporated molecules from the often complex aerosol mixture. Hence, AMS is non-selective, and the fragmentation strongly limits the analysis of single compounds in the mass spectra. GC/MS (the standard method for quantification of airborne organics) on the other hand can only quantify 10-20 % of the total OA mass.

Compound Classes Measured with AMS

The AMS mass spectra often is comprised of complex mixtures of compounds, which enables measurements of compound classes rather than specific molecules. The SP-AMS was applied to measure different compound classes in aerosol particles. An example of aerosol mass spectra from cookstove emissions divided into compound classes is shown in the left panel of Figure 9. The marker ions of levoglucosan and other anhydrous sugars ($C_2H_4O_2^+$ and $C_3H_5O_2^+$)[132] (Paper I) are shown in purple. The marker ions for methoxy phenols (Paper I), denoted phenols, are shown in orange. The following marker ions for methoxy phenols were included in the analysis $C_7H_7O^+$, $C_7H_5O_2^+$, $C_8H_9O^+$, $C_8H_9O_2^+$, $C_8H_7O_3^+$, $C_9H_{11}O_2^+$, $C_9H_{11}O_3^+$, $C_9H_9O_4^+$, and $C_{10}H_{13}O_3^+$.[133]

Ten parent ions of unsubstituted particle phase PAHs in the m/z range 200-300 were included in the AMS analysis (Papers I and II), in line with Herring et al.[134]

Quantification of the total organic aerosol was performed according to the standard method, with an RIE of 1.4 in dual vaporizer mode in unit mass resolution (Paper I) and in high resolution (Paper II). The quantification is based on the repeatability of electron ionization and the approximation that organic compounds possess equal ionization efficiencies. However, a large variability in the RIE of organic aerosol has been demonstrated depending on the chemical composition of the organic particles.[135] As a consequence, thorough calibration is needed for measurements of a specific marker compound (class).

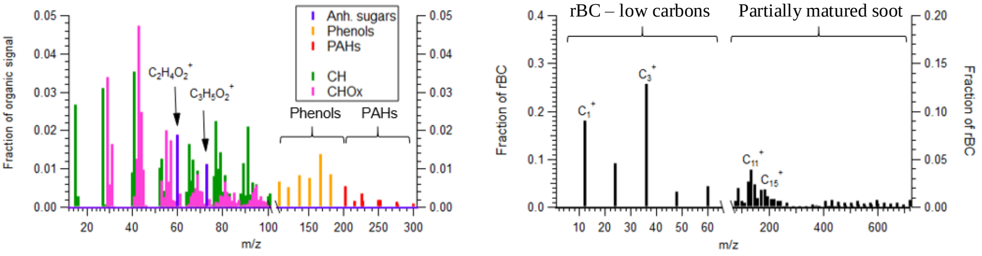

Figure 9 Organic mass spectrum (left panel) divided into the compound classes: anhydrous sugar marker ions (purple), phenols marker ions (orange), PAH marker ions (red). The spectrum also shows the remaining organic ions: the CH fragments (green) and the oxygenated ions (pink), which both have contributions from the defined compound classes as well as unidentified compounds. The right panel shows the carbon ions with C_1^+-C_5^+ showing rBC, and carbon fragments larger than C_5^+ showing the partially matured soot. Both high resolution spectra were measured with the SP-AMS in dual vaporizer mode.

The carbon ions of refractory black carbon (rBC) C_1^+-C_5^+, which represent mature soot, are shown in the right panel of Figure 9. rBC was quantified by C_3^+ scaled to eBC measurements (Papers I and II), further described in Paper I. Partially matured soot is estimated from the sum C_6^+-C_{59}^+.[136]

Inorganic phosphate salts from the candle wicks were measured in Paper II. The following ions were added as a HR family and included in the analysis: PO, HPO, PO_2, HPO_2, PO_3, HPO_3, PO_4, HPO_4, and H_2PO_4.

Online Measurements of DEHP Uptake on Particles

For the quantitative measurements of DEHP in Papers III and IV, the AMS was calibrated with pure DEHP particles, generated by the particle generator as described on page 38. Equation 4 was used to calculate the RIE relative to nitrate, (Figure 8). RIE equals 5.0 in AMS 1, the instrument that was applied in Paper IV, and RIE equals 4.3 in AMS 2, which additionally was applied in Paper III. The signal fraction of the ion $C_5H_8O_3^+$ (m/z 149) in the pure DEHP mass spectrum was found to be 5.9%. These two numbers were used to calculate the mass concentration of DEHP in both Papers III and IV. The ion $C_5H_8O_3^+$ is not specific for DEHP; it is a marker ion for phthalate esters. However, in Paper III, the mass concentration was dominated by DEHP. Other phthalate esters, which may be omnipresent in the laboratory environment, will therefore be minor compared to DEHP, and consequently, the measured concentration is attributed to DEHP. In Paper IV, the interference from omnipresent phthalates was avoided by using deuterium-labeled DEHP.

Offline Analysis with GC/MS/MS

For the gas-phase and particle phase PAH analysis in Paper II and the phthalate air analysis in Paper IV, tandem MS (GC-MS/MS) with a triple quadrupole mass analyzer was used, which is a highly sensitive and selective method for quantification at trace level. More details are provided in the respective Papers. GC/MS is the standard method for the identification and quantification of volatile and semi-volatile organic compounds. GC/MS is applicable for quantitative measurements of specific marker compounds for organic aerosol of a minor fraction of the organic aerosols, in contrast to the AMS measurements, which provide information about the entire organic aerosol.

Determining Emission Factors

Emission factors (EFs) were calculated in Papers I and II. Emission factors in $\mathrm{g/kg_{dry\ fuel}}$ provide information that together with data on fuel consumption, can be applied to evaluate the overall mass of pollutants emitted to the atmosphere. The emission factors presented in Paper I were calculated by use of the carbon mass balance method (equation 5), assuming that the carbon mass from the fuel is emitted as CO and CO_2.[45, 137]

$$EF_i\left(\frac{\mathrm{g}}{\mathrm{kg}_{dry\,fuel}}\right) = \frac{C_i}{\Delta CO + \Delta CO_2} \cdot f_C \qquad (5)$$

EF_i is the emission factor of a compound (class) i, C_i is the concentration of a compound (class), ΔCO and ΔCO_2 are the concentrations (in g carbon m^{-3}) of CO and CO_2, respectively, where background concentrations have been subtracted, and f_c is the carbon fraction in the dry fuel.

Emission factors (or emission rates) per time unit, were calculated for the candle emissions from stressed burning (Paper II). Emission factors enable estimations of concentrations in specific indoor environments by assuming burn time, number of candles, air exchange rate, loss rate, and the volume of the room where the candles are burned. Emission factors may be applied by modelers in exposure assessments. In Paper II, a simplified expression derived from He et al.[138] was applied to calculate emission factors according to equation 6.

$$S_{av}(\frac{\mu g}{h}) = \frac{C_{av} \cdot V \cdot (a + k)}{n} \tag{6}$$

with S_{av} being the emission factor per candle in units of µg/h, C_{av} is the average measured concentration, V is the volume, n is the number of candles, a is the measured air exchange rate, and k is the loss rate of particles, mainly caused by coagulation (number concentration) and wall losses (number and mass concentration). This simplified expression can be applied because steady state conditions are reached quickly, compared to the length of the experiment, with the high air exchange rate of 2 h^{-1}.

The loss rate, k, was derived by the expression in equation 7,[138] and calculated from decay experiments.

$$a + k = \frac{1}{t} \frac{\ln(C_t)}{\ln(C_0)} \tag{7}$$

where t is the time and C_0 and C_t are the initial concentration and concentration at time t, respectively.

Ethical Considerations

Conducting the human exposure study (Paper IV) was subject to ethical considerations. Prior to the start of the exposures, ethical approval was obtained from the The Ethical Committee at Lund University (Dnr. 2016/130) in accordance with the Declaration of Helsinki.

Before the start of exposures, detailed information about the purpose of the study was formulated and provided to the participants, both as written and oral information. Participation was voluntary and participants were ensured that they could stop their participation at any time. Signed consent from the participants was obtained before the start of the exposures.

The recruitment of participants was carried out by advertisements for voluntary participants in the Lund University area outside of the department where the research group is based. Symbolic compensation was provided to the participants. This was balanced to compensate participants for any inconvenience and to ensure that there was no economic incentive to participate in the study.

Metabolites were measured in urine samples collected 24 hours after exposure as often as possible. No invasive biological samples were taken. Participants were informed about the storage of urine samples in the biobank, and their right to change their storage consent at any time.

The following inclusion criteria were used for all participants:

- They had to be healthy and above the age of 18.
- They did not have any airway diseases, eczema, open wounds, or were smokers.
- They were not pregnant or planning pregnancy within the time frame of the exposures.
- Before exposure, all participants went through a medical examination, and were continuously observed by a medical doctor throughout the entire exposure time.

An exposure concentration of 300 µg m^{-3} for three hours was chosen because this was considered adequate to enable measurements of metabolite after short-term exposure. In comparison, the current occupational 8-hour average exposure limit value is 3 mg m^{-3}. In 10 Swedish homes, the total phthalate concentrations in air were measured in the interval 1.2 to 7.4 µg m^{-3}, with a median of 2.7 µg m^{-3}.[139] Thus, an exposure to 300 µg m^{-3} for three hours corresponds to breathing in a Swedish home for 13 days with a phthalate concentration of 2.7 µg m^{-3}. Furthermore, the exposure to DEP and DEHP has been found to occur mainly through ingestion.[88] A daily exposure to eight common phthalates was estimated to be about 7.5 µg per kg bodyweight for adults.[88] By assuming an average breathing rate of 7.5 l min^{-1} and a bodyweight of 60 kg for women, and 9.5 l min^{-1} and 80 kg for men at 300 µg m^{-3}, the maximum internal exposure is 6.8 and 6.1 µg per kg bodyweight, respectively. Thus, the exposure is comparable to an average total daily dose of phthalates. It is the ubiquitous continuous exposure to phthalates that is of concern. Consequently, no health effects were expected from the 3-hour short-term exposure.

Data protection, privacy and confidentiality in the personal data collection and processing were handled in accordance with EU legislation. The participants' identity will not be revealed at any stage of the research project.

Results and Discussion

Indoor Air Pollution from Combustion Sources

Cookstoves

Thermochemical Conversion Framework

The simplified thermochemical conversion framework, described in Paper I and shown in Figure 10, was developed and applied to interpret and categorize the chemical properties of the aerosol emissions from four cookstoves of different advancement. The framework is focused on the key particle emission classes measured with high time-resolution with the SP-AMS. It also includes the gas-phase compounds benzene, toluene, and xylenes (BTX), as these are major precursors of PAHs and soot and of relevance for SOA formation. It is inspired by the literature on pyrolysis of lignocellulosic biomass, summarized on page 25. The framework concentrates on the thermochemical processing of cellulose and lignin, which are the main components of woody biomass and the main contributors to emissions of condensed phase compounds at ambient conditions. Hemicellulose tends to decompose to higher volatility products during pyrolysis,[79, 81, 140] with a lower contribution to the condensed phase, and is therefore not accounted for in the framework.

Upon pyrolysis, cellulose decomposes into anhydrous sugars and lignin decomposes into phenolic compounds, among others. These two emission classes constitute the primary pyrolysis products in the framework. Secondary and tertiary pyrolysis products are grouped together in the simplified framework and referred to as "converted pyrolysis products". This class includes the gas-phase compounds BTX and particle phase PAHs. These are formed from further thermochemical conversion of anhydrous sugars and phenolic compounds, among others. Thus, primary and converted pyrolysis classes are subclasses of organic aerosol.

Upon further thermochemical conversion and sufficiently high temperatures, soot formation processes can occur. The soot formation region is constituted of partially matured soot, which are particles that are intermediate of inception and fully matured soot. These particles have undergone some high-temperature aging but are not fully carbonized.[27] The end product in the framework is mature soot denoted refractory Black Carbon (rBC).

Overall, the framework consists of six classes: 1) anhydrous sugars, 2) phenols, 3) BTX in the gas-phase, 4) particle phase PAHs, 5) partially matured soot, 6) rBC. Emissions of CO_2, CO, methane, and other gas-phase compounds are not explicitly accounted for in the framework. Emissions from combustion systems strongly depend on thermochemical parameters such as temperature, residence time, air to fuel ratio, and mixing or spatial distribution in the fuel bed, which are not accounted for in the framework.

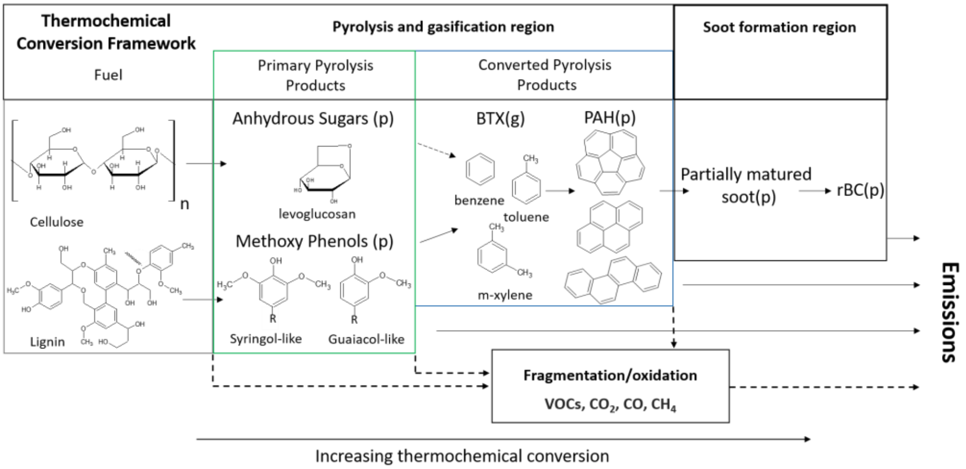

Figure 10 The thermochemical conversion framework includes emission classes that can be measured with high time-resolution with SP-AMS and FTIR. It describes the thermochemical conversion of the lignocellulosic biomass components, cellulose and lignin, under pyrolysis conditions, as well as the subsequent conversion for the formation of condensable organic compounds and soot. The framework comprises the compounds that were measured in Paper I, and does not account for all possibly formed products.

The thermochemical conversion framework was validated by carrying out a correlation analysis of the different particle emission classes for the highly time-resolved SP-AMS data for the 3-stone fire and the rocket stove, which is reported in Paper I. The analysis of both stoves showed a strong correlation between the anhydrous sugars and phenols. Correlations with other emission classes were reduced gradually for emission classes associated with increased thermochemical conversion. PAHs correlated with partially mature soot, and partially mature soot correlated with rBC. These results support the concept of the framework.

Emission Factors

The emission factors (EFs) from the four different cookstoves studied in Paper I are shown in Figure 11. The upper panel shows the EFs of each of the six emission classes included in the thermochemical conversion framework as well as EFs of organic aerosol (OA), secondary organic aerosol (SOA), and the sum of OA and rBC reported as PM_1. The EFs of anhydrous sugars, phenols, and partially matured soot are given as normalized signal intensity per $kg_{\text{dry fuel}}$ because of limitations in the quantification of these emission classes.

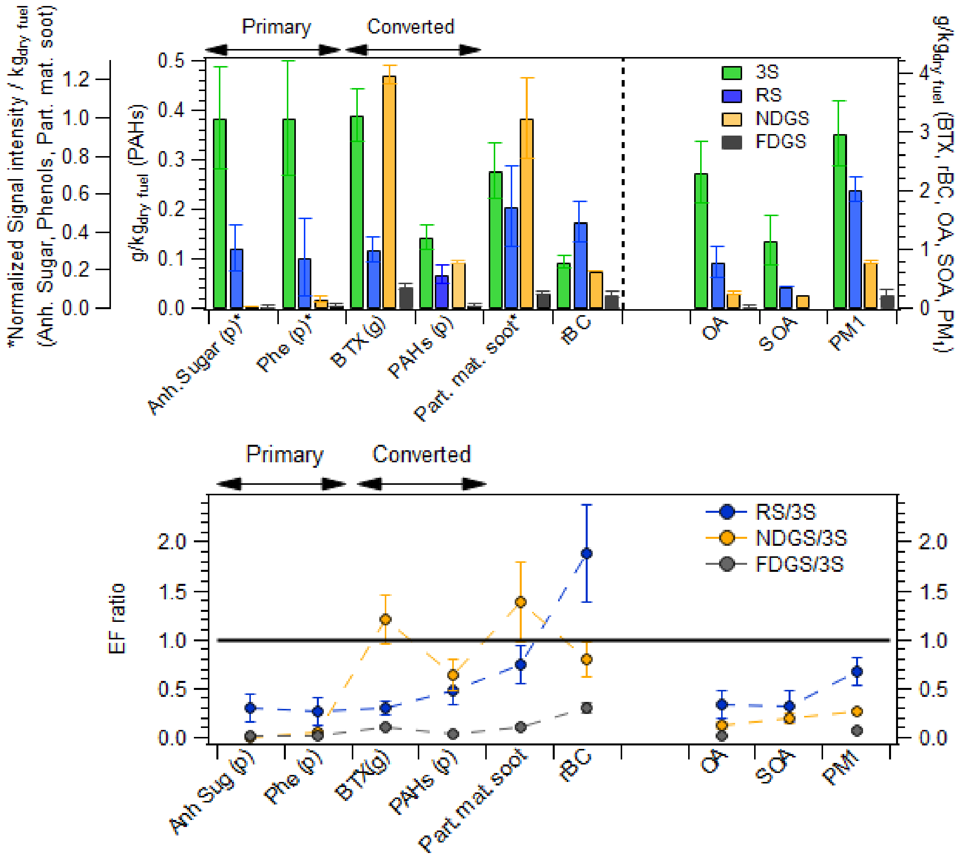

Figure 11 The upper panel shows emission factors of the 3-stone fire (3S), rocket stove (RS), natural draft gasifier stove (NDGS), and forced draft gasifier stove (FDGS) for the different emission classes in the thermochemical conversion framework. Note the different scales for the emission classes: anhydrous sugars, phenols, and partially matured soot are all reported as normalized signal intensity on the left axis. PAHs are shown on the primary left axis, and BTX, rBC, OA, SOA, and PM_1 on the right axis. The lower panel shows the emission factor (EF) ratios of the emission classes for the RS, NDGS, and FDGS relative to the the 3S.

The EF ratios of each emission class relative to the 3-stone fire are shown in the lower panel in Figure 11. The 3-stone fire showed high emissions of the primary pyrolysis products (anhydrous sugars and phenols) and high emissions of the converted pyrolysis products (BTX and PAHs). The high emissions of primary and converted pyrolysis products were associated with an overall low degree of thermochemical conversion. In comparison to the 3-stone fire, the improved rocket stove showed lower emissions of both primary and converted pyrolysis products, but higher rBC emissions. This is in line with the added insulation in the rocket stove design (compared to the 3-stone fire), which increases the temperature and improves mixing of air and combustion gases. Hence, the emissions of primary and converted pyrolysis products were reduced. The increased rBC emissions may be partly caused by quenching of the flame, which leads to cooling of the flame and reduced soot oxidation.

The advanced natural draft gasifier stove (NDGS), on the other hand, showed low emissions of the primary pyrolysis products and the overall highest emissions of BTX and high emissions of PAHs (converted pyrolysis products). It also showed the highest emissions of partially matured soot, but reduced rBC emissions compared to the 3-stone fire and rocket stove. This was associated with an increased thermochemical conversion relative to the 3-stone fire and rocket stove, but not high enough to fully transform the converted pyrolysis products and partially matured soot into rBC. The high emissions of converted pyrolysis products were attributed to insufficient secondary air supply from the natural draft, compared to the volatilized combustion gases, causing air starved regions, in particular at the center of the stove as air is consumed in the outer regions. In the air starved regions low temperature combustion conditions may occur, which delays the conversion of the converted pyrolysis products (BTX and PAHs) and partially matured soot into rBC.[141]

The forced draft gasifier stove (FDGS) showed a strong reduction of all emission classes compared to the 3-stone fire and showed the overall lowest emissions of the four tested stoves. This is in accordance with the stove design, which instead of natural draft, utilizes an electrically powered fan for the secondary air supply. This creates better mixing of combustion gases and air, and minimizes air starved regions. Thus, these combustion conditions favor soot formation and soot oxidation processes, i.e. a rapid conversion of BTX, PAHs, and partially matured soot into rBC. Hence, the emissions of carcinogenic organic compounds are reduced.

Most of these findings are supported by the literature. The reduction of $PM_{2.5}$ emissions and increased rBC emissions observed from a rocket stove relative to a traditional 3-stone fire is in line with other studies that compare the two stoves.[44, 142, 143] The reduction of $PM_{2.5}$ emissions from improved stoves and the increasing emissions of other co-pollutants, such as PAHs, as a result of certain design features has previously been observed.[44] Significant reductions of all emission classes by the FDGS has similarly been observed in $PM_{2.5}$, OC, EC, and CO emissions from a gasifier pellet stove of the FDGS type examined in Paper I compared to traditional stoves in field measurements.[45]

Moreover, the results showed that elevated OA emissions were associated with emissions of primary pyrolysis products (anhydrous sugars and phenols), and to a lower degree with emissions of converted pyrolysis products (BTX and PAHs). On the other hand, SOA emissions were associated with both primary and converted pyrolysis products. These trends were also supported by data from a Nordic heating stove, further described in Paper I. Partially matured soot correlated with PAHs and with rBC according to the correlation analysis described in Paper I. The occurrence of partially matured soot was associated with high PAH to rBC ratios (Figure 11).

The overall reductions in the emission classes of relevance for health – BTX, PAHs, and rBC – were not reduced in the same proportion as PM_1. Inorganic compounds are not included in PM_1, and constituted a low fraction (5-10 %) of PM_1. Reduction in PM_1 was caused by significant decreases in OA and primary pyrolysis products. Moreover, reduction in PM_1 can still imply high BTX, PAH and rBC emissions.

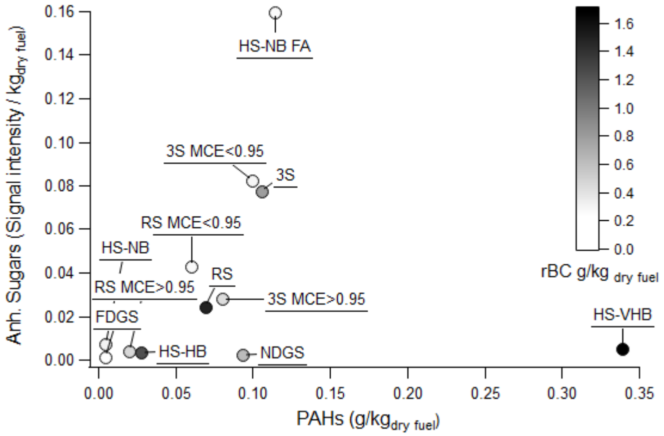

Figure 12 Anhydrous sugars, a marker of primary pyrolysis products vs. PAHs(p), a marker of converted pyrolysis products for the cookstoves and the Nordic heating stove. Heating stoves are labeled HS. The results are color coded according to rBC emissions, with a darker color indicating higher rBC emissions.

Figure 12 displays the anhydrous sugars (a marker for primary pyrolysis products) plotted against PAHs (a marker for converted pyrolysis products) color coded with respect to rBC emissions. The figure also includes fuel addition (MCE<0.95) and intermediate flaming (MCE>0.95) burn phases for the 3-stone fire and rocket stove. It also includes data from a Nordic heating stove, further explained in Paper I.

Anhydrous sugars, PAHs, and rBC are all correlated poorly. Hence, rBC is not a good proxy for primary pyrolysis products (represented by anhydrous sugars) and converted pyrolysis products (represented by PAH emissions) and vice versa.

Figure 12 also illustrates the similarly low emissions of all three emission classes from the FDGS cookstove and the Nordic heating stove operated at nominal burn rate (NB). It is worth noting from a human exposure perspective, because the emissions from the Nordic heating stove are required to always be emitted throughout the building via a chimney, in contrast to cookstoves which are used indoors by 92 % of the population in Kenya,[47] mostly without any chimney. Human exposure to cookstove emissions are further compared and discussed on page 60.

Comparisons of the 3-stone fire and rocket stove with the NDGS and FDGS are limited by the use of different fuels: casuarina softwood (logs/sticks) for the 3-stone fire and the rocket stove, and mixed pine and spruce (softwood pellets) in some cases mixed 50:50 with bagasse and coffee husk for both of the gasifier stoves. The applied fuel was identical for both of the gasifier stoves. A further limitation in the comparison of emissions between the stoves is the high ash content in bagasse and coffee husk used as fuel in the gasifier stoves, which can affect the burn rate and thereby the emissions of all emission classes within the framework.

Candles

Emission Factors of Compounds from Stressed Burning of Candles

The emission factors (Paper II) of particle and gas compounds from stressed burning of the five types of pillar candles of different wax and wick composition (Table 1), as well as emission factors from one steady burn experiment of candle 1 are presented in Table 2. For comparison, literature data on candle emissions are provided in

Table 3 for stressed and steady burn conditions. Only a few other studies of candle emissions report emission factors for stressed burning conditions. The literature on candle emissions from steady burn are available; they represent ideal burn conditions. However, occupant activities in residences are known to cause fluctuations in air velocities,[144] which may result in stressed burn conditions.

The results generally showed large variability between the candle emissions of soot (eBC/EC), particle phase PAHs, and $PM_{2.5}$, and to a lower degree variability of organic carbon (OC), inorganic particle components, and particle number concentration (PNC). Low variability among candles was observed for the emission factors of NO_x, formaldehyde, and gas-phase PAHs. Candle 5 showed the highest emissions of $PM_{2.5}$, eBC/EC, particle phase PAHs, and slightly higher NO_x, while candle 4 had the lowest emissions of these compounds, followed by candle 3.

In Paper II, candle 5 showed by far the highest $PM_{2.5}$ emission factor of 3 mg/h and candles 1 and 4 showed the lowest of 0.3 mg/h, based on gravimetric measurements. In comparison, PM emission factors in the interval of 7.6-26.6 mg/h have been reported in other laboratory studies for stressed burning.[64-66] The particle number emission factors from Paper II (Table 2) are at the same order of magnitude but slightly higher compared to values reported by Zai et al.[66] (stressed burn), by Manoukian et al. (steady burn)[145], and by Klosterköther et al. (steady burn).[146] Differences in the measured particle sizes varied among studies, which limits the comparison. Particle number concentrations in Paper II were measured in the size interval 2.4-914 nm, while Zai et al. reported numbers for the interval 10-500 nm.[66] Particle number concentrations from candles have previously been reported to be significant at sizes below 10 nm.[147]

Table 2 Emission factors per candle from stressed burning of candles 1, 2, 3, 4, and 5 and one steady burn experiment for candle 1. The emission factors from offline analysis ($PM_{2.5}$, EC, OC, inorganics, particle phase PAHs (p), gas-phase PAHs (g), and formaldehyde [CH_2O]) are reported from 0.5-3.5 hours and the emission factors from online analysis (PNC, eBC, and NO_x) are reported from 0-3.5 h.

	$PM_{2.5}$* µg/h	EC* µg/h	OC* µg/h	Inorg* µg/h	PNC[c] Particles/h	eBC µg/h	PAH* ng/h	PAH* ng/h	NO mg/h	NO_2 mg/h	CH_2O* µg/h
					2.4-914 nm		(p)	(g)			
Candle1	276	328	86	90	9.3×10^{13}	340	73	734	2.5	0.9	53
Candle2	518	380	104	128	9.0×10^{13}	528	90	721	3.8	1.2	45
Candle3	397	259	138	28	6.3×10^{13}	274	59	708	3.1	1.0	43
Candle4	328[a]	35[b]	52	69	8.5×10^{13}	132	24[b]	1251	2.9	1.0	49
Candle5	3041	3128	225	52	1.5×10^{13}	3622	577	669	4.3	1.3	39
Steady1	<DL	<DL	134		8.3×10^{13}	3	26	1015	2.8	0.6	35

[a] Value based on one measurement

[b] Possibly underestimated value, as the peak emissions occurring within first half hour are not included (sampling 0.5-3h)

[c] Emission factors of PNC based on 3h average concentrations (i.e. 0-3 h of the experiments), due to use of the catalytic stripper in the last 30 minutes of the experiment.

It should be noted that the stressed burning conditions in the three other studies in Table 3 may differ from the conditions applied in Paper II, as no air velocities were reported. Furthermore, the candle shapes differ, for example tapered candles were used in other studies, some of which had added pigments, versus white pillar candles used in Paper II. The method for calculating emission factors may also have differed. These differences limit the basis for direct comparisons. Thus, the decreased particle mass and number emissions reported in Paper II compared to the literature may reflect the influence of the candle shape, the composition of raw materials (wax and wick), as well as the burning conditions on the emissions.

The emission factors of $PM_{2.5}$ and eBC from steady burn reported by Stabile et al.[148] are notably similar to or even higher than the emission factors of $PM_{2.5}$ and eBC from candles 1-4 (Table 2). Emission factors of PAHs have only been reported for the steady burn conditions of candles. The upper values of the sum of particle- and gas-phase PAH emissions reported by Derudi et al. for steady burn conditions are lower than the total PAH emissions for all candle types reported in Table 2.

Higher BC emissions can be expected at stressed burning compared to steady burn conditions, as flickering of the flame at increased air velocities causes poorer conditions for full soot oxidation, see page 24. The comparisons above of aerosol emissions reported in Paper II with literature on stressed and steady burn of candles may well reflect the improvements incorporated in candle design (raw materials, shape) by the manufacturers in the past decade. However, it may also reflect, that the level of stressing of the candle flames applied in Paper II was less intense.

Table 3 Literature values reported on candle emissions

Candle type	PNC Particles/h	PM mg/h	BC/EC mg/h	PAH ng/h	Reference	Burn mode
				(g+p)		
Red paraffin (t)	$1.05 \pm 0.24 \cdot 10^{13}$ (10-500 nm)	7.61 ± 2.25 (0.1-10 µm)			Zai et al.[66]	Stres.
Stearine (t)		8.9 ± 0.4 ($PM_{2.5}$)	4.5 ± 0.2 (EC)		Pagels et al.[64]	Stres.
Blue stearine +parffin (t)		25.3 ± 0.02 ($PM_{2.5}$)	19.0 ± 0.6 (EC)		Pagels et al.[64]	Stres.
Paraffin church candle		26.6 (up to 1.8 µm)	24.1 (EC)		Fine et al.[65]	Stres.
paraffin (t)		0.87 ($PM_{2.5}$)	0.74 (BC)		Stabile et al.[148]	Steady
Scented besswax + vegetable oil (c)	$2.0 \pm 0.1 \cdot 10^{13}$				Manoukian et al.[145]	Steady
Paraffin (c)		0.01-0.73 (PM_1)		74-289	Derudi et al.[149]	Steady
Paraffin	$3.0\text{-}6.9 \cdot 10^{13}$ (7-1000 nm)	0.24-0.99 (15-1000 nm)			Klosterköther et al.[146]	Steady

(t) tapered candle

(c) container candle

Derudi et al. reported emission factors of NO_x in the range of 1.7-2.5 mg/h. Klosterköther et al. reported NO of 2.7-3 mg/h and NO_2 of 1.8-2.1 mg/h, for steady burn of paraffin container candles and paraffin church candles, respectively.[146, 149] For comparison, emission factors of NO_x 3.4-5.6 mg h^{-1}, NO 2.5-4.3 mg h^{-1}, and NO_2 0.9-1.3 mg h^{-1} were found for stressed burn in Paper II. Hence, the studies measured lower or comparable NO_x, but Klosterköther et al.[146] measured higher NO_2 emissions compared to Paper II.

Klosterköther et al. also reported formaldehyde emissions of 18-27 µg/h from steady burn of paraffin church candles,[146] in comparison to values of 35 µg/h for steady burn of candle 1 and 39-53 µg/h in Paper II for stressed burn (Table 2), which are around twice as high. Formaldehyde is classified as a group I (carcinogenic to humans) by IARC.

Key results from Paper II are presented in Figure 13. They show strong short-lived peaks of rBC emitted from the stressed candle flame measured above the flame. The figure illustrates the co-emission of rBC, OA, and PAHs at stressed burn conditions. It further shows that rBC constituted approximately 95% of the particle mass and OA around 5% in each of the peak emissions (based on the sum of rBC, OA and PAHs). Additionally, NO_x did not show any clear trends related to the flickering of the flame. High temperatures are necessary for the formation of thermal NO_x; consequently, reduced temperatures caused by flickering can be expected to result in opposite trends for BC and NO_x. However, this was only apparent in some cases, as seen in Figure 13.

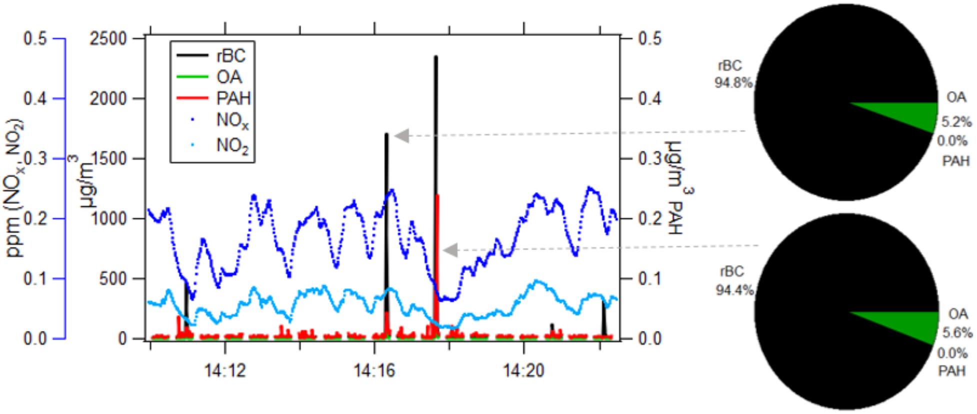

Figure 13 AMS time trace of emissions of OA, rBC, and PAHs, as well as NO_x and NO_2 time traces. Example of candle 5 above the flame measurements. The graph supports the the coemisssion of rBC, OA, and PAHs, while NO_x does not follow a similar pattern. The pie charts show the percentage distribution of rBC, OA, and PAHs in the two peaks as the sum of the three components based on mass concentration.

The emissions from the stressed burning of candles showed very high soot (eBC/ rBC/EC) emissions and low particle phase PAHs relative to soot. In line with the thermochemical conversion framework (Figure 10) presented for cookstoves, the combustion conditions in the candle flame favor a rapid conversion of BTX (not measured) and PAHs into mature soot (rBC). Hence, a low particle phase PAH to soot ratio is observed from candle emissions. High rBC emissions occurred when the candle flame was disturbed and cooled down by the surrounding air flow. The soot oxidation was limited by reduced flame temperatures and residence time in the flame. On the contrary, emissions after extinguishing the candles (Figure 4 in Paper II) showed high concentrations of organic aerosol and low to moderate emissions of rBC and particle phase PAHs.

The AMS mass spectrum from the smouldering emissions after extinguishing (Figure 6 in Paper II) showed organic peaks at m/z 60 ($C_2H_4O_2^+$) and m/z 73 ($C_3H_5O_2^+$). These signals have traditionally been associated with levoglucosan and anhydrous sugars from cellulose from biomass pyrolysis.[132] The candle wick material is made of cotton (pure cellulose). The AMS signal at m/z 60 and m/z 73 has also previously been measured from cooking aerosol.[25, 150]

Number and mass size distributions were measured for the stressed burning of candles and one steady burn experiment for candle 1 (Paper II). The particle number size distributions for all candles were dominated by ultrafine particles (UFPs) with modes between 5-8 nm. Candle 5 had an additional mode at 217 nm. The mass size distributions for candles 1-4 were bimodal with modes between 27-44 and 533-914 nm. Candle 5 on the other hand, was unimodal with a mode at 573 nm. The UFP number concentrations were similar for candles 1-4 and lowest for candle 5 (Paper II).

The UFPs emitted from candles 1-4 were associated with inorganic salts from the wick impregnation.[64] This was further supported by the correlations that were found between inorganic emission factors and UFP mass ($PM_{0.1}$), and that there were no strong correlations between eBC and EC with UFP mass observed (Paper II). Additionally, data from application of a catalytic stripper supported this (Paper II). The comparison of mass concentrations showed that eBC made up the largest proportion of PM emissions (comparison of eBC with mass concentration derived from SMPS (Paper II)). For candles 1-4, inorganic compounds constituted 8-20% of the mass concentration, while for candle 5, it was only around 1%.

The results from Paper II provide emission factors of health relevant particle and gas components, studied under controlled stressed burning conditions. An intercomparison of the five candles studied in Paper II showed significant variations in the emissions of soot, $PM_{2.5}$, and particle phase PAHs among the candle types. This demonstrates the influence of the wax and wick composition on the particle emissions. On the contrary, the gas-phase compounds NO_x, formaldehyde, and PAHs did not show a clear reduction by varying the wax and wick composition. In addition, the measurements of rBC, OA, and particle phase PAHs were highly correlated, which indicates that they may be applied as proxies for one another, while NO_x has to be measured separately.

Uptake of Phthalates on Aerosol Particles

Figure 14 displays a key result from Paper III. It shows the DEHP mass fraction, in percentage, on laboratory-generated ammonium sulfate particles, and on the indoor aerosols that were measured after passing the 1.2 L chamber equipped with PVC flooring, described in details in the method section. It thereby shows the $K_{gas\text{-}particle} \times y_0$ in equation 1 in percentage. The mass fraction of DEHP on the particles increased with increasing residence time of the particles in the chamber for all particle types. It further shows a higher sorption of DEHP on indoor particles with an organic fraction, than on inorganic ammonium sulfate particles that did not pass the thermodenuder. The organic aerosol content of these ammonium sulfate particles was 0.8% by mass. Moreover, it shows that the indoor particles and ammonium sulfate particles (with no removal of volatile impurities) had a higher sorption of DEHP compared to when they were denuded, where a large proportion of organic and inorganic volatile components were removed.

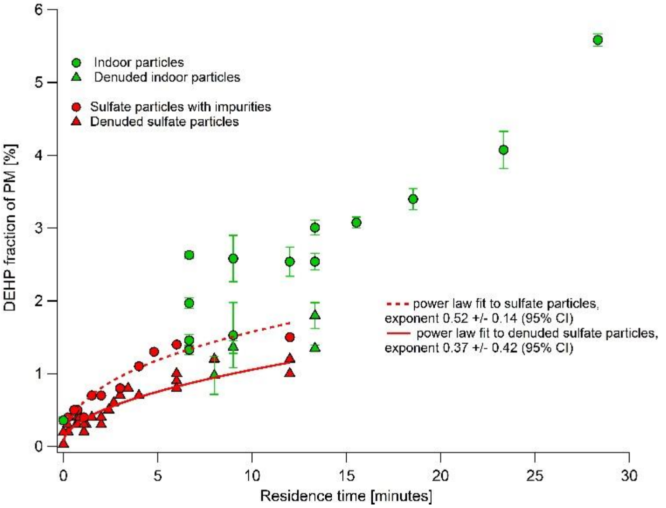

Figure 14 DEHP mass fraction of the particles measured after passing the chamber equipped with PVC flooring plotted against the residence time of the particles in the chamber. The plot contains indoor particles (green circles), sulfate particles with impurities (red circles), and denuded particles where some impurities were removed of each of the respective particle types (triangles).

This indicates two different mechanisms of uptake, namely *ad*sorption of DEHP on the ammonium sulfate particle surfaces, and *ab*sorption of DEHP in the organic particle phase. The sorption of DEHP may also occur by a combination of both uptake mechanisms, with the importance of *ab*sorption increasing with an increase in the concentrations of organics in the particles, and the importance of *ad*sorption increasing when the volatile fraction has been removed from the particles. This is in line with the results of Wu et al.[21] who reported an order of magnitude higher sorption of DEHP to pure oleic acid particles and squalene particles than to ammonium sulfate particles. Furthermore, a higher sorption into oleic acid particles was observed compared to squalene particles.[21] The results may also depend on the surface area mass ratio of the particle types, which was not addressed in Paper III.

The size-resolved data in Paper III showed variation in DEHP sorption across the particle diameter. A higher DEHP mass fraction was measured in the ultrafine particles, which also had a higher mass fraction of organic aerosol compared to larger particle sizes. Inorganic particles were shifted towards larger particle diameters.

The sorption of reduced nitrogen species on particles in indoor environments from nicotine, attributed to protonation/deprotonation, has previously been measured with AMS.[151] This is another process governing the uptake of chemicals on aerosol particles.

The presence of particles of itself can increase the emission rate of DEHP from materials such as PVC,[13] which also was observed in Paper III. The presence of aerosol particles thus increases the total mass available for uptake, which has been observed in occupied residences.[152] Based on the Paper III results, this effect may be especially important for indoor aerosols with a large fraction of non-polar organic components. The particle phase may thereby increase the amount of DEHP available for uptake in the body. Recently, the increased phthalate concentration in particles was measured during cooking events, with high emissions of organic aerosol, in residential settings. The particle phase phthalate concentrations were attributed to emissions from PVC flooring in the residence.[153]

The importance of DEHP sorption to particles in human uptake depends on the DEHP particle phase concentration relative to the DEHP gas-phase concentration. Based on the vapor pressure of DEHP at 25°C, the gas-phase concentration saturates at approximately 1 µg m^{-3},[13, 108] and maximum at 3 µg m^{-3}.[114] The gas-phase concentration saturates before the particle phase concentration, and in indoor environments, the gas-phase concentration of DEHP can consequently exceed the particle phase concentration of DEHP. Taking into account the average deposition fraction of 26% of the particle size distribution reported in Paper IV, and assuming 100% deposition in the airways of the gas-phase DEHP, the concentration of particles would thereby have to be 4 times higher than the gas-phase concentration to exceed the human uptake by mass due to gas-phase DEHP. This assumes particle size distributions that are similar to those used in Paper IV. However, the presence of particles in proximity to DEHP sources can contribute to an increased airborne concentration of DEHP and thereby increased airborne exposure to DEHP.

Human Uptake of Gas-Phase and Particle Phase Phthalates

The key results from the human exposure study (Paper IV) of deuterium-labeled DEP and DEHP (hereafter referred to as DEP and DEHP) are presented in Figure 15. It shows the measured uptake by inhalation and dermal exposure by air to skin transfer of DEHP and DEP normalized to body weight, air concentration, and time of exposure. The results show a higher uptake of inhaled DEP in the gas-phase, than by inhaled DEHP in the particle phase. This result reflects the difference in deposition of particles and gases in the airways, disregarding any differences in chemical properties of DEP and DEHP. The deposition of particles in the airways was estimated by the MPPD model,[154] and showed an average deposited fraction of 26 % of the inhaled mass of DEHP for the given size distribution. When particles that contain SVOCs are inhaled, some SVOCs may evaporate rapidly from the particle upon inhalation due to heating and will thereby be absorbed in the airways as gas molecules. Given the timescale of seconds the particles spend in the airways before deposition, the upper estimate for this effect is 10% for the size distribution applied in the exposure study (Paper IV). This estimation is based on measurements of the evaporation of dioctyl phthalate (which is the straight chain isomer of DEHP) from particles, where the evaporation timescale is minutes to hours.[155, 156]

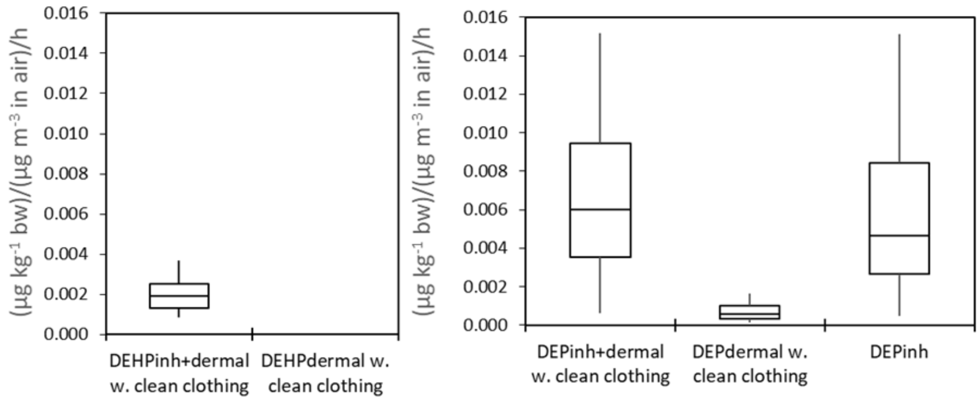

Figure 15 Uptake of DEHP (panel A) and DEP (panel B) in the four exposure scenarios. The uptake is normalized to body weight, air concentration, and time of exposure. The inhalation-only uptake of DEP is calculated by subtracting the dermal uptake from the combined uptake of inhalation+dermal. The plots show the median, 25, and 75 percentiles of the uptake, and the whiskers denote maximum and minimum values. DEHPdermal with clean clothing was below the detection limit.

No dermal uptake during the three hours of exposure to DEHP was detected. That means the metabolite concentrations in the urine samples were below the detection limit of 0.1-0.9 ng/mL (metabolite dependent).[157] Furthermore, the dermal uptake of DEP was 10 times lower compared to the uptake of DEP by inhalation. The participants were wearing clothing that never had been exposed to deuterium-labeled phthalates. The effect of clothing on dermal uptake was investigated in a study of nicotine transfer from cigarette smoke by Bekö et al.[158] The dermal uptake was studied while some participants wore clean clothing and showered, and compared to dermal uptake by bare skin and by wearing contaminated clothing. The comparison indicated that wearing clean clothing was a means of protection, while wearing contaminated clothing resulted in an accelerating effect on the dermal uptake of nicotine. Moreover, showering seemed to reduce the uptake of phthalates.[158] However, the influence of clothing and showering are dependent on the physicochemical properties of the SVOCs. Thus, the results presented in Paper IV may represent minimal dermal uptake as opposed to the study by Weschler et al.,[125] where the dermal uptake was maximized by exposing bare skinned participants.

In real-life situations, clothing may be pre-exposed to DEHP and DEP in the storage time between washing and wearing it again. However, for DEHP this would most likely have a minor effect considering the concentrations of the DEHP measured in dwellings or personal air samples that are in the order of nanograms to a few micrograms per cubic meter.[159] Cao et al. estimated equilibrium times for DEHP on clothing to 9400 h at 25°C, that is, more than one year.[121] Clothing may also contain phthalates from the manufacturing process, which has been reported in Chinese infant clothing.[160] The effect of dermal exposure by contact transfer from DEHP deposited on clothing thus depends on the indoor DEHP concentration, on the length of storing clothing after washing, and pre-contamination in the manufacturing process. The equilibrium time for DEP could be considerably lower, for which the pre-exposure of clothing may make up a meaningful exposure.[161] How much of the DEP and DEHP that is removed in the laundry process depends on the temperature of the water, the detergent, and if the clothes are tumble dried at high temperature. DEP may be removed more easily than DEHP.[162]

In the study in Paper IV, the skin surface that was not covered with clothing was on the hands. The surface area of the hands is approximately 1/20 of the entire skin surface area of a person's body. A full body is approximately 1.8 m^2 and hands are approximately 0.09 m^2.[88] In a study by Weschler et al. on DEP uptake, similar inhalation and dermal uptakes were observed when the participants were exposed wearing only shorts.[125] Figure 16 shows the results from Weschler et al.[125] on DEP uptake normalized to body weight, air concentration, and time of exposure. When the results by Weschler et al. are compared to the results of Paper IV, the median uptake of DEP by inhalation is in agreement within the range of uncertainty, 0.005±0.005, in our study compared to 0.007 (µg kg-1 bw)/(µg m-3 in air)/h in the Weschler et al. study.[125] For the dermal uptake, the median uptake is 0.0006±0.0005 in our study and 0.008 (µg kg-1 bw)/(µg m^{-3} in air)/h in the Weschler et al. study. These numbers reflect a difference in the study design: wearing clean clothing and showering after exposure vs. being bare-skinned under exposure and not showering after.

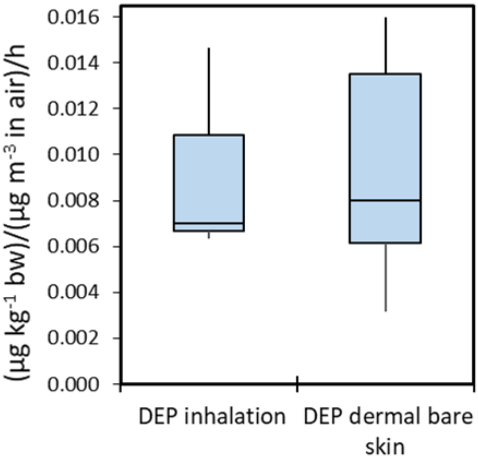

Figure 16 The box plot shows the uptake of DEP by inhalation and dermal uptake with bare skin by Weschler et al.[125] The uptake is normalized to body weight, air concentration, and time of exposure. The plot shows the median, 25, and 75 percentiles of the uptake, and the whiskers denote the 10th and 90th percentiles.

Estimation of Possible Indoor Air Exposures Calculated Based on EFs

Cookstove Exposure Scenario

Emission factors from the cookstoves studied in Paper I were used to estimate exposure concentrations in an average home in a developing country. WHO has set an annual average guideline for $PM_{2.5}$ of 10 µg/m^3, and a 24-hour average guideline for CO of 7 mg/m^3. The $PM_{2.5}$ interim guidelines IT-3 15 µg/m^3, IT-2 25 µg/m^3, and IT-1 35 µg/m^3 were published to provide incremental steps in meeting the guidelines in areas where concentrations are high and a reduction to the guideline concentrations within a short time is unrealistic. These concentrations are set on the basis of an air exchange rate (AER) of 15 h^{-1}, a kitchen area of 30 m^3, and a daily burn time of 4 hours.[163]

The above described assumptions, together with the emission factors, were used to estimate the concentrations of PAHs, rBC, OA, PM_1, and CO in homes during a cooking event with the application of one of the four cookstoves, described in Paper

I. For the calculations, the assumption of 1 kg wood consumed per 1-hour cooking event using the 3-stone fire and the rocket stove, and 0.5 kg pellets per 1-hour cooking event using the NDGS and FDGS were applied. The fuel consumptions have been measured for a 3-stone fire and a FDGS, the latter of which is identical to the FDGS used in the Paper I field study.[45] Thus, the calculated concentrations for the RS may be overestimated, and the concentrations for the NDGS may be underestimated

Table 4 Estimated indoor concentrations per hour assuming an AER of 15 h^{-1} in a 30 m^3 kitchen with 1 kg of wood consumed for 3-stone fire (3S) and rocket stove (RS), and 0.5 kg of wood consumed for the NDGS and FDGS. The particle classes are based on SP-AMS measurements.

	PAH µg/m³	**rBC µg/m³**	**OA µg/m³**	**PM_1 µg/m³**	**CO mg/m³**
3S	240	1800	5100	6900	110
RS	150	3300	1800	5000	57
NDGS	100	700	300	990	40
FDGS	5	260	35	300	6

The estimated air concentrations of particle phase PAHs, rBC, OA, PM_1, and CO for a cooking event provided in Table 4 represent short-term exposures during one cooking event lasting for 1 hour. Real cooking events are likely to occur several times a day and may even last longer. As a consequence of the high air exchange rate of 15 h^{-1} the pollutant concentrations will reach steady state rapidly as well as decrease rapidly after the cooking event when there is no active point source.

Based on the estimated concentrations in Table 4, the CO peak emission of the FDGS does not exceed the WHO 24-hour average guideline for a CO of 7 mg/m^3 and would according to the applied assumptions and estimations meet the guideline criteria for CO. The peak emissions of NDGS would also meet the guideline's 24-hour average, when assuming four daily cooking events of 1-hour duration and negligible background CO concentrations; whereas the rocket stove and 3-stone fire would exceed the guideline criteria with these assumptions. However, the estimated PM_1 concentrations for all stoves exceed the annual $PM_{2.5}$ IT-1 35 µg/m^3, by assuming 4-hours daily cooking and negligible background concentrations. However, other sources such as traffic emissions are likely to further contribute to the $PM_{2.5}$ exposure. The particle phase PAH emissions from all stoves, and in particular from the 3-stone fire, RS, and NDGS are very high. For comparison, the highest total PAH concentration (including gas-phase PAHs) measured in Swedish restaurant kitchens was ~1 µg/m^3.[164] These concentrations are based on a rough estimation that in turn is based on the assumptions and criteria described above. Concentrations in real life are strongly dependent on the duration of cooking events, air exchange rate, fuel properties, and stove operation conditions.

Candle Exposure Scenario

The emission factors reported in Paper II were applied in equation 6 to calculate room concentrations that may occur in a 90 m^2 home after burning five candles for 3.5 hours. Concentrations of $PM_{2.5}$, EC, NO_2, PAHs in the gas-phase and in particles, and the PAH concentrations reported as BaP eq were calculated (Table 5). The home was assumed to be 90 m^2 with a ceiling height of 2.4 m (volume of 216 m^3), and an air exchange rate of 0.5 h^{-1}. The particle mass decay rate, k in equation 7, mainly attributed to particle wall losses was assumed to be 0.5 h^{-1}. This slightly higher value compared to the calculated value of 0.4 h^{-1} in the 21.6 m^3 chamber in Paper II, was chosen to account for larger surface area available for deposition in homes. The loss rate of 0.5 h^{-1} was also assumed for the gas-phase PAHs. The volume represents a home with open doors, assuming the candle emissions are uniformly mixed throughout the volume. At an air exchange rate of 0.5 h^{-1} and a k value of 0.5 h^{-1}, the concentrations of emitted pollutants, after the candles are lit, will increase over time until reaching steady state. Once the candles are extinguished, the concentrations will decrease over time. The concentrations reported in Table 5 are reached after 3.5 hours and are not constant within the 3.5 hours.

Table 5 Estimated concentrations from emission factors in a 90 m^2 home after 3.5 hours of burning five candles at stressed burn conditions with an air exchange rate of 0.5^{-1}. The concentrations are calculated based on the emission factors in Table 2. The PAHs are provided on the basis of GC-MS measurements.

	$PM_{2.5}$ µg m^{-3}	EC µg m^{-3}	NO_2 µg m^{-3}	$PAH_{particle}$ ng m^{-3}	PAH_{gas} ng m^{-3}	$PAH_{particle+gas}$ ng m^{-3}	BaP $eq_{particle+gas}$ ng m^{-3}
Candle 1	6	8	27	1.7	17.0	18.7	0.02
Candle 2	12	9	32	2.1	16.7	18.8	0.02
Candle 3	9	6	27	1.4	16.4	17.8	0.02
Candle 4	8	0.8	26	0.6	29.0	29.5	0.01
Candle 5	70	72	38	13.4	15.5	28.8	0.10

The total PAH concentrations for the five candles are comparable to the concentrations reported in urban outdoor and indoor air in Gothenburg,[165, 166] and in Swedish restaurant kitchens.[164] The BaP eq concentrations in Table 5 are in the range of 0.01-0.1 ng/m^3 summed over gas-phase and particle phase PAHs. Gustafson et al.[167] measured gas-phase and particle phase PAHs in homes in a Swedish village during winter. The BaP eq PAH mean concentrations were found to 1.00 ng/m^3 (median 0.88 ng/m^3) in homes with wood stoves, 0.28 ng/m^3 (median 0.23 ng/m^3) in homes without wood stoves and, 0.67 ng/m^3 (median 0.74 ng/m^3) outdoors.[167] WHO has set an air quality guideline that estimates a unit risk estimate of BaP eq concentration of 0.1 ng m^{-3}, which will cause an added cancer risk of 1/100,000.[36]

The $PM_{2.5}$ concentrations were calculated to be between 6-70 µg/m^3. The WHO air quality guidelines for $PM_{2.5}$ are 25 µg/m^3 as a 24-hour average and 10 µg/m^3 as a yearly average.[36] Even the highest concentration of 70 µg/m^3 with a burn time of 3.5 hours will not exceed the 24-hour average guideline.

The EC concentrations in the candle exposure scenario were in the range of (0.8) 6-72 µg/m^3. It should be noted that the EC measurement (resulting in a concentration of 0.8 µg/m^3) for candle 4 is biased low because of the chosen sampling time and the emission profile of candle 4, further described in Paper II. In a study from Belgium, the average personal BC exposure concentrations during daily activities have been measured to range from 1.2 µg/m^3 during sleep to 6.4 µg/m^3 in transport.[168] In Stockholm, the highest average personal BC exposure concentrations averaged over the transport time have been measured up to 2.7 µg/m^3 during bus transportation.[169] Compared to these exposure concentrations, even the lowest calculated EC concentration of 6 µg/m^3 from the stressed candle burning of candle 3 is likely to contribute to peak exposures of EC.

The estimated NO_2 concentrations were in the range of 26-38 µg/m^3. The WHO indoor guideline of NO_2 is 200 µg/m^3 as an 1-hour average concentration, and 40 µg/m^3 as an annual average.[36] The estimated NO_2 concentrations from stressed burning of candles in the given exposure scenario will not exceed the WHO guidelines.

In summary, the estimated concentrations of $PM_{2.5}$ and NO_2 in the candle exposure scenario do not exceed the WHO guidelines. However, candle burning is not the only source contributing to exposure to these pollutants. This means that the stressed burning of candles will add to the cumulative exposure of $PM_{2.5}$, EC, NO_2, and PAHs.

It is important to note that the stressing of the candles presented here and in Paper II represent a scenario with continuous stressing of the flame. In real-life exposures, scenarios with less, intermediate, and higher levels of the stressing can occur.

The resulting exposure concentration to particles and gases from the stressed burning of candles strongly depends on the number and type of candles, burn time, volume of indoor environments, and air exchange rate. The exposure scenario presented here was chosen to represent a possible scenario of burning candles in a home. The number of candles burned in homes will vary. Burning five candles at a time may be a low estimate during the Christmas season, but may be suitable at other times of the year. Burning of fewer candles could also be considered. Situations with even more intense burning can also occur. It is, for instance, common to burn candles in the bathroom in a significantly smaller volume where doors most often are kept closed. It is not uncommon in restaurants that each table is decorated with one or more burning candles. Thus, 15-20 candles can be burned in a volume similar to the presented scenario where air movements are influenced by guests entering and leaving, opening doors, speaking and breathing in near proximity to the candle, and from staff continuously walking around to serve the guests. The exposure concentrations can therefore be considerably higher than in the scenario concentrations in Table 5.

The toxicity of candle soot particles is not well explored. Inflammation and cytotoxicity of the lung[170] as well as telomere shortening in the lung and spleen, a marker for risk of developing cardiovascular diseases,[171] have been reported from animal studies. Other studies on health effects from exposure to candle emissions have shown reduced cognitive abilities in humans[172] and negative changes in lung function.[173] Soot emitted from the burning of candles possess a similar morphology to soot from diesel engine exhaust, with similar primary particle size but a larger mobility diameter.[64] Diesel engine exhaust, including both particles and gases, is classified as a group I carcinogen by IARC. Consequently, exposure to candle soot may be of health concern, but there is a need for further elucidation of the toxicity of candle soot.

Conclusions

In this thesis, the physicochemical characterization and quantification of emissions from various indoor aerosol sources were performed, from cookstoves, candles, and DEHP emissions from PVC flooring. Indoor exposure scenarios were estimated on the basis of calculated emission factors of the studied cookstoves and candles. A human exposure study was also conducted of the dermal and inhalation uptake of DEHP (exposure route via particles) and DEP (exposure route via gas-phase).

A simplified thermochemical conversion framework was applied for the interpretation of aerosol emissions from four cookstoves and a Nordic wood log stove for residential heating (Paper I). The framework was validated by a correlation analysis between the emission classes measured with high time-resolution SP-AMS. The results showed that OA was mainly associated with primary pyrolysis products. SOA on the other hand was associated with both primary and converted pyrolysis products. These results indicate that markers of primary pyrolysis products, converted pyrolysis products, and soot particles should preferably be measured for a more complete evaluation of the primary and secondary particle emissions. Moreover, measurements of some of these emission classes may be used for estimating the prevalence of other emission classes not measured.

The PM_1 mass emission factors from cookstoves decreased with the increasing technological advancement of the cookstoves. However, the reduction in emissions of the carcinogens and classes of known health and climate concern – BTX, PAHs, and rBC – did not decrease in the same proportion as PM_1 for the improved and advanced cookstoves. Emissions from improved and advanced cookstoves may thus also result in elevated emissions of aerosol components of concern for human health.

In a simplified exposure scenario, exposure concentrations in homes were estimated from the derived emission factors. Based on this estimation with assumptions of fuel consumption, air exchange rate, volume of the room, and burn time, the forced draft gasifier stove fulfilled the interim guideline for CO, but none of the cookstoves studied fulfilled the $PM_{2.5}$ emission annual average interim guideline set by WHO.

The physicochemical properties and emission levels were measured from candle burning in an environmental laboratory chamber under simulated stressed burn conditions. A wide range of particle and gas-phase emissions were measured from the stressed burning of candles with different wax and wick compositions. Large variabilities in $PM_{2.5}$ mass, BC, and particle phase PAH emissions were measured between the five candle types. Large variations in the particle emissions over time were also found between the candle types. Particle emission levels thereby depend on the time duration candles are burned. In all cases the stressed burning of candles was dominated by BC emissions on a mass concentration basis. The candles with the lowest BC emission showed high emissions of ultrafine particles, with a high probability of depositing in the alveolar region upon inhalation. In contrast to BC, NO_x emissions did not show great variation between the different candle types. Due to thermal NO_x formation at high temperature conditions, reduction of NO_x is difficult to obtain by introducing changes in the candle design, and NO_x may be inevitable from candle burning. No clear reductions in formaldehyde and gas-phase PAHs were observed by changes in the wax and wick composition. Measurements directly above the candle flame at stressed burn conditions showed correlations between rBC, PAHs, and organic aerosol emissions, which indicates that they may be used as proxies for each other.

The extinguish emissions (smouldering) were also measured above the flame, which as expected showed high organic aerosol emissions relative to rBC. Markers of anhydrous sugars, usually associated with the pyrolysis of cellulose in biomass burning, were observed in the AMS spectra of extinguish smoke. Markers of anhydrous sugars emitted from candles have not been observed previously, and were attributed to pyrolysis products from the cotton (cellulose) wick.

Based on an estimated exposure scenario of candle burning in a home, stressed burning of the lowest emitting candle in this research may even contribute to relatively high peak exposures of EC, PAHs (BaP eq), $PM_{2.5}$, and NO_2, and may be a contributor to personal exposure to these pollutants.

AMS was applied for novel *in-situ* measurements of particle phase phthalates, which are present at trace amounts indoors. It was demonstrated that the mass fraction of DEHP sorbed to the particles depends on the particle characteristics. (Paper III). A higher sorption was measured on indoor particles with higher organic mass fractions compared to laboratory-generated ammonium sulfate particles. Size-resolved data showed higher mass fractions of DEHP on ultrafine particles that had a higher mass fraction of organic aerosols. The emission rate of DEHP from PVC flooring increased in the presence of high particle concentrations, as previously reported by others. This implies that indoor particles increase the airborne concentration (gas + particle) of DEHP and other SVOCs. In indoor environments, where organic aerosol concentrations often are high, sorption of SVOCs on particles may be significant. This highlights the importance of reducing the semi-volatile and health hazardous chemicals in consumer products and indoor air particle concentrations.

The dermal and inhalation uptake in humans of two common phthalates from airborne exposure was evaluated in a human exposure study. A novelty consisted of the use of deuterium-labeled phthalates for airborne exposure, which allowed the exclusion of interference from omnipresent phthalates. The results showed both dermal and inhalation uptake of gas-phase DEP in participants wearing clean clothing, with higher uptake via inhalation. Uptake via air-to-skin-transfer of DEP was ten times lower than the inhalation uptake, with participants wearing clean clothing and showering after exposure. No dermal uptake of DEHP particles was quantified. A higher uptake was measured of gas-phase DEP compared to particle phase DEHP via inhalation. This demonstrates the difference in the uptake of particles and gases, without considering any differences in the chemical properties between DEP and DEHP.

The emission factors reported in this thesis can be applied by modelers to assess exposure to health-relevant emissions, such as PAHs and soot, from specific sources in indoor environments. The results presented in this thesis emphasize the need of considering the physicochemical properties of particles and of SVOCs for adequate exposure and risk assessments in indoor environments. Moreover, the need for a more complete evaluation of their impact on human health.

Outlook

Some knowledge gaps for future research became apparent in the research process. Measurements of air pollution in parts of the world that strongly depend on biomass cookstoves are generally limited. In particular, time-resolved measurements of chemical composition are limited, partly caused by infrastructural limitations, for instance unstable electricity. Future work on the thermochemical conversion framework should aim at evaluating its applicability in estimating the prevalence of other emission classes not measured. This may be useful in for instance field measurements of few emission classes that represent markers of primary pyrolysis products, converted pyrolysis products, and soot. Furthermore, interdisciplinary research with a holistic approach is needed that combines the existing knowledge from laboratory tests of aerosol emissions from cookstoves with considerations of norms, cultural practices, and the design of cookstoves.

Studies characterizing candle emissions in residential settings are limited and are needed for proper exposure assessments of gas and particle emissions from candles. Introducing standardized measurement protocols for the assessment of emissions from stressed candle burning, to regulate the candle manufacturing, may help reducing air pollutants emitted from candles.

The effect of the gas-particle partitioning of SVOCs and what it means for human exposures to SVOCs in indoor environments is generally not well understood. Measurements in both model setups as well as in real indoor environments are needed to increase the understanding of SVOCs adsorption/absorption on/in particles and the importance for human exposures. Furthermore, environmental factors such as relative humidity and the effect on the gas-particle partitioning of SVOCs is not well understood.

The influence of wearing clean clothing and showering after exposure on the uptake by air-to-skin transfer of DEP, DEHP, and other SVOCs is not properly elucidated. Clean clothing and showering seem to render protection from dermal uptake of airborne phthalates, and clothing contaminated with certain chemicals enhance the dermal uptake. How these two extremes translate into real life conditions needs further research.

Generally, the understanding of the effects of particle composition on $PM_{2.5}$ toxicity is inadequate; in particular the toxicity of organic aerosol is not well understood.

Additionally, the effect on toxicity of the sorption of SVOCs to particles relative to the particle core composition is not well known. Future studies that aim to identify the most health harmful components inhaled in indoor environments can help in coming up with mitigation strategies.

Acknowledgements

I thank my supervisors Joakim Pagels, Aneta Wierzbicka, Axel Eriksson, and Annette Krais for advice and support throughout the thesis work. Financial support from the Swedish Research Councils VR (Dnr 2018-04200), FORMAS (Dnr 2013-01023, Dnr 216-2013-1478, and Dnr 216-2013-1966), and the Innovation Fund Denmark (File No. 7048-00002A.) is greatly acknowledged.

References

1. Cosselman, K. E.; Navas-Acien, A.; Kaufman, J. D. Environmental factors in cardiovascular disease. *Nat. Rev. Cardiol.* **2015,** *12* (11), 627-42.
2. Clark, N. A.; Demers, P. A.; Karr, C. J.; Koehoorn, M.; Lencar, C.; Tamburic, L.; Brauer, M. Effect of Early Life Exposure to Air Pollution on Development of Childhood Asthma. *Environ. Health Perspect.* **2010,** *118* (2), 284-290.
3. Shiraiwa, M.; Selzle, K.; Poschl, U. Hazardous components and health effects of atmospheric aerosol particles: reactive oxygen species, soot, polycyclic aromatic compounds and allergenic proteins. *Free. Radic. Res.* **2012,** *46* (8), 927-39.
4. Landrigan, P. J.; Fuller, R.; Acosta, N. J. R.; Adeyi, O.; Arnold, R.; Basu, N.; Baldé, A. B.; Bertollini, R.; Bose-O'Reilly, S.; Boufford, J. I.; Breysse, P. N.; Chiles, T.; Mahidol, C.; Coll-Seck, A. M.; Cropper, M. L.; Fobil, J.; Fuster, V.; Greenstone, M.; Haines, A.; Hanrahan, D.; Hunter, D.; Khare, M.; Krupnick, A.; Lanphear, B.; Lohani, B.; Martin, K.; Mathiasen, K. V.; McTeer, M. A.; Murray, C. J. L.; Ndahimananjara, J. D.; Perera, F.; Potočnik, J.; Preker, A. S.; Ramesh, J.; Rockström, J.; Salinas, C.; Samson, L. D.; Sandilya, K.; Sly, P. D.; Smith, K. R.; Steiner, A.; Stewart, R. B.; Suk, W. A.; van Schayck, O. C. P.; Yadama, G. N.; Yumkella, K.; Zhong, M. The Lancet Commission on pollution and health. *The Lancet* **2017**.
5. Shrivastava, M.; Cappa, C. D.; Fan, J.; Goldstein, A. H.; Guenther, A. B.; Jimenez, J. L.; Kuang, C.; Laskin, A.; Martin, S. T.; Ng, N. L.; Petaja, T.; Pierce, J. R.; Rasch, P. J.; Roldin, P.; Seinfeld, J. H.; Shilling, J.; Smith, J. N.; Thornton, J. A.; Volkamer, R.; Wang, J.; Worsnop, D. R.; Zaveri, R. A.; Zelenyuk, A.; Zhang, Q. Recent advances in understanding secondary organic aerosol: Implications for global climate forcing. *Rev. Geophys.* **2017,** *55* (2), 509-559.
6. Bond, T. C.; Doherty, S. J.; Fahey, D. W.; Forster, P. M.; Berntsen, T.; DeAngelo, B. J.; Flanner, M. G.; Ghan, S.; Kärcher, B.; Koch, D.; Kinne, S.; Kondo, Y.; Quinn, P. K.; Sarofim, M. C.; Schultz, M. G.; Schulz, M.; Venkataraman, C.; Zhang, H.; Zhang, S.; Bellouin, N.; Guttikunda, S. K.; Hopke, P. K.; Jacobson, M. Z.; Kaiser, J. W.; Klimont, Z.; Lohmann, U.; Schwarz, J. P.; Shindell, D.; Storelvmo, T.; Warren, S. G.; Zender, C. S. Bounding the role of black carbon in the climate system: A scientific assessment. *J. Geophys. Res. Atmospheres* **2013,** *118* (11), 5380-5552.
7. Smith, K. R.; Bruce, N.; Balakrishnan, K.; Adair-Rohani, H.; Balmes, J.; Chafe, Z.; Dherani, M.; Hosgood, H. D.; Mehta, S.; Pope, D.; Rehfuess, E. Millions Dead: How Do We Know and What Does It Mean? Methods Used in the Comparative Risk Assessment of Household Air Pollution. *Annu. Rev. Public Health* **2014,** *35* (1), 185-206.

8. World Health Organization (WHO) Household air pollution and health. http://www.who.int/mediacentre/factsheets/fs292/en **2016**.

9. Kassotis, C. D.; Vandenberg, L. N.; Demeneix, B. A.; Porta, M.; Slama, R.; Trasande, L. Endocrine-disrupting chemicals: economic, regulatory, and policy implications. *The Lancet Diabetes & Endocrinology* **2020,** *8* (8), 719-730.

10. Kahn, L. G.; Philippat, C.; Nakayama, S. F.; Slama, R.; Trasande, L. Endocrine-disrupting chemicals: implications for human health. *The Lancet Diabetes & Endocrinology* **2020,** *8* (8), 703-718.

11. Frederiksen, H.; Jørgensen, N.; Andersson, A.-M. Correlations Between Phthalate Metabolites in Urine, Serum, and Seminal Plasma from Young Danish Men Determined by Isotope Dilution Liquid Chromatography Tandem Mass Spectrometry. *J. Anal. Toxicol.* **2010,** *34* (7), 400-410.

12. Hauser, R.; Skakkebaek, N. E.; Hass, U.; Toppari, J.; Juul, A.; Andersson, A. M.; Kortenkamp, A.; Heindel, J. J.; Trasande, L. Male Reproductive Disorders, Diseases, and Costs of Exposure to Endocrine-Disrupting Chemicals in the European Union. *J. Clin. Endocrinol. Metab.* **2015,** *100* (4), 1267-1277.

13. Benning, J. L.; Liu, Z.; Tiwari, A.; Little, J. C.; Marr, L. C. Characterizing gas-particle interactions of phthalate plasticizer emitted from vinyl flooring. *Environ. Sci. Technol.* **2013,** *47* (6), 2696-703.

14. Klepeis, N. E.; Nelson, W. C.; Ott, W. R.; Robinson, J. P.; Tsang, A. M.; Switzer, P.; Behar, J. V.; Hern, S. C.; Engelmann, W. H. The National Human Activity Pattern Survey (NHAPS): a resource for assessing exposure to environmental pollutants. *J. Expo. Sci. Environ. Epidemiol.* **2001,** *11* (3), 231-252.

15. Brasche, S.; Bischof, W. Daily time spent indoors in German homes – Baseline data for the assessment of indoor exposure of German occupants. *Int. J. Hyg. Environ. Health* **2005,** *208* (4), 247-253.

16. Weschler, C. J.; Carslaw, N. Indoor Chemistry. *Environ. Sci. Technol.* **2018,** *52* (5), 2419-2428.

17. Lai, A. C. Particle deposition indoors: a review. *Indoor air* **2002,** *12* (4), 211-214.

18. Wang, C.; Collins, D. B.; Arata, C.; Goldstein, A. H.; Mattila, J. M.; Farmer, D. K.; Ampollini, L.; DeCarlo, P. F.; Novoselac, A.; Vance, M. E.; Nazaroff, W. W.; Abbatt, J. P. D. Surface reservoirs dominate dynamic gas-surface partitioning of many indoor air constituents. *Science Advances* **2020,** *6* (8), eaay8973.

19. Nazaroff, W. W. Indoor particle dynamics. *Indoor air* **2004,** *14*, 175-183.

20. Weschler, C. J.; Nazaroff, W. W. Semivolatile organic compounds in indoor environments. *Atmos. Environ.* **2008,** *42* (40), 9018-9040.

21. Wu, Y.; Eichler, C. M. A.; Cao, J.; Benning, J.; Olson, A.; Chen, S.; Liu, C.; Vejerano, E. P.; Marr, L. C.; Little, J. C. Particle/Gas Partitioning of Phthalates to Organic and Inorganic Airborne Particles in the Indoor Environment. *Environ. Sci. Technol.* **2018**.

22. Eichler, C. M. A.; Hubal, E. A. C.; Xu, Y.; Cao, J.; Bi, C.; Weschler, C. J.; Salthammer, T.; Morrison, G. C.; Koivisto, A. J.; Zhang, Y.; Mandin, C.; Wei, W.; Blondeau, P.; Poppendieck, D.; Liu, X.; Delmaar, C. J. E.; Fantke, P.; Jolliet, O.; Shin, H. M.; Diamond, M. L.; Shiraiwa, M.; Zuend, A.; Hopke, P. K.; von Goetz,

N.; Kulmala, M.; Little, J. C. Assessing Human Exposure to SVOCs in Materials, Products, and Articles: A Modular Mechanistic Framework. *Environ. Sci. Technol.* **2021,** *55* (1), 25-43.

23. Salthammer, T.; Zhang, Y.; Mo, J.; Koch, H. M.; Weschler, C. J. Assessing human exposure to organic pollutants in the indoor environment. *Angew. Chem. Int. Ed. Engl.* **2018**.

24. Thatcher, T. L.; Lunden, M. M.; Revzan, K. L.; Sextro, R. G.; Brown, N. J. A Concentration Rebound Method for Measuring Particle Penetration and Deposition in the Indoor Environment. *Aerosol Sci. Technol.* **2003,** *37* (11), 847-864.

25. Omelekhina, Y.; Eriksson, A.; Canonaco, F.; Prevot, A. S. H.; Nilsson, P.; Isaxon, C.; Pagels, J.; Wierzbicka, A. Cooking and electronic cigarettes leading to large differences between indoor and outdoor particle composition and concentration measured by aerosol mass spectrometry. *Environ. Sci. Process. Impacts* **2020,** *22* (6), 1382-1396.

26. Farmer, D. K.; Vance, M. E.; Abbatt, J. P. D.; Abeleira, A.; Alves, M. R.; Arata, C.; Boedicker, E.; Bourne, S.; Cardoso-Saldana, F.; Corsi, R.; DeCarlo, P. F.; Goldstein, A. H.; Grassian, V. H.; Hildebrandt Ruiz, L.; Jimenez, J. L.; Kahan, T. F.; Katz, E. F.; Mattila, J. M.; Nazaroff, W. W.; Novoselac, A.; O'Brien, R. E.; Or, V. W.; Patel, S.; Sankhyan, S.; Stevens, P. S.; Tian, Y.; Wade, M.; Wang, C.; Zhou, S.; Zhou, Y. Overview of HOMEChem: House Observations of Microbial and Environmental Chemistry. *Environ. Sci. Process. Impacts* **2019,** *21* (8), 1280-1300.

27. Michelsen, H. A.; Colket, M. B.; Bengtsson, P.-E.; D’Anna, A.; Desgroux, P.; Haynes, B. S.; Miller, J. H.; Nathan, G. J.; Pitsch, H.; Wang, H. A Review of Terminology Used to Describe Soot Formation and Evolution under Combustion and Pyrolytic Conditions. *ACS Nano* **2020,** *14* (10), 12470-12490.

28. Patel, M. M.; Chillrud, S. N.; Correa, J. C.; Hazi, Y.; Feinberg, M.; Kc, D.; Prakash, S.; Ross, J. M.; Levy, D.; Kinney, P. L. Traffic-related particulate matter and acute respiratory symptoms among New York City area adolescents. *Environ. Health Perspect.* **2010,** *118* (9), 1338-43.

29. Cornell, A. G.; Chillrud, S. N.; Mellins, R. B.; Acosta, L. M.; Miller, R. L.; Quinn, J. W.; Yan, B.; Divjan, A.; Olmedo, O. E.; Lopez-Pintado, S.; Kinney, P. L.; Perera, F. P.; Jacobson, J. S.; Goldstein, I. F.; Rundle, A. G.; Perzanowski, M. S. Domestic airborne black carbon and exhaled nitric oxide in children in NYC. *J. Expo. Sci. Environ. Epidemiol.* **2012,** *22* (3), 258-66.

30. Grahame, T. J.; Klemm, R.; Schlesinger, R. B. Public health and components of particulate matter: the changing assessment of black carbon. *J. Air Waste Manag. Assoc.* **2014,** *64* (6), 620-60.

31. Petzold, A.; Ogren, J. A.; Fiebig, M.; Laj, P.; Li, S. M.; Baltensperger, U.; Holzer-Popp, T.; Kinne, S.; Pappalardo, G.; Sugimoto, N.; Wehrli, C.; Wiedensohler, A.; Zhang, X. Y. Recommendations for reporting "black carbon" measurements. *Atmos. Chem. Phys.* **2013,** *13* (16), 8365-8379.

32. Bolling, A. K.; Sripada, K.; Becher, R.; Beko, G. Phthalate exposure and allergic diseases: Review of epidemiological and experimental evidence. *Environ. Int.* **2020,** *139*, 105706.

33. Boström, C.-E., Gerde, P., Hanberg, A., Jernström, B., Johansson, C., Kyrklund, T., Rannug, A., Törnqvist, M., Victorin, K., Westerholm, R. Cancer risk assessment, indicators, and guidelines for polycyclic aromatic hydrocarbons in the ambient air. *Environ. health persp.* **2002,** *110*, 451-488.

34. Jameson, C. W. Polycyclic aromatic hydrocarbons and associated occupational exposures. *IARC* **2010,** *161*.

35. Raub, J. A.; Mathieu-Nolf, M.; Hampson, N. B.; Thom, S. R. Carbon monoxide poisoning—a public health perspective. *Toxicology* **2000,** *145* (1), 1-14.

36. World Health Organization WHO guidelines for indoor air quality: selected pollutants. **2010**.

37. Loomis, D.; Guyton, K. Z.; Grosse, Y.; El Ghissassi, F.; Bouvard, V.; Benbrahim-Tallaa, L.; Guha, N.; Vilahur, N.; Mattock, H.; Straif, K. Carcinogenicity of benzene. *The Lancet Oncology* **2017,** *18* (12), 1574-1575.

38. Filley, C. M.; Halliday, W.; Kleinschmidt-Demasters, B. K. The Effects of Toluene on the Central Nervous System. *J. Neuropathol. Exp. Neurol.* **2004,** *63* (1), 1-12.

39. Huang, Y.; Unger, N.; Storelvmo, T.; Harper, K.; Zheng, Y.; Heyes, C. Global radiative effects of solid fuel cookstove aerosol emissions. *Atmospheric Chem. Phys.* **2018,** *18* (8), 5219-5233.

40. Roden, C. A.; Bond, T. C.; Conway, S.; Osorto Pinel, A. B.; MacCarty, N.; Still, D. Laboratory and field investigations of particulate and carbon monoxide emissions from traditional and improved cookstoves. *Atmos. Environ.* **2009,** *43* (6), 1170-1181.

41. Heft-Neal, S.; Burney, J.; Bendavid, E.; Burke, M. Robust relationship between air quality and infant mortality in Africa. *Nature* **2018**.

42. Jetter, J.; Zhao, Y.; Smith, K. R.; Khan, B.; Yelverton, T.; Decarlo, P.; Hays, M. D. Pollutant emissions and energy efficiency under controlled conditions for household biomass cookstoves and implications for metrics useful in setting international test standards. *Environ. Sci. Technol.* **2012,** *46* (19), 10827-34.

43. Wathore, R.; Mortimer, K.; Grieshop, A. P. In-Use Emissions and Estimated Impacts of Traditional, Natural- and Forced-Draft Cookstoves in Rural Malawi. *Environ. Sci. Technol.* **2017,** *51* (3), 1929-1938.

44. Bilsback, K. R.; Dahlke, J.; Fedak, K. M.; Good, N.; Hecobian, A.; Herckes, P.; L'Orange, C.; Mehaffy, J.; Sullivan, A.; Tryner, J.; Van Zyl, L.; Walker, E. S.; Zhou, Y.; Pierce, J. R.; Wilson, A.; Peel, J. L.; Volckens, J. A Laboratory Assessment of 120 Air Pollutant Emissions from Biomass and Fossil Fuel Cookstoves. *Environ. Sci. Technol.* **2019,** *53* (12), 7114-7125.

45. Champion, W. M.; Grieshop, A. P. Pellet-Fed Gasifier Stoves Approach Gas-Stove Like Performance during in-Home Use in Rwanda. *Environ Sci Technol* **2019**.

46. Bhattu, D.; Zotter, P.; Zhou, J.; Stefenelli, G.; Klein, F.; Bertrand, A.; Temime-Roussel, B.; Marchand, N.; Slowik, J. G.; Baltensperger, U.; Prevot, A. S. H.; Nussbaumer, T.; El Haddad, I.; Dommen, J. Effect of Stove Technology and

Combustion Conditions on Gas and Particulate Emissions from Residential Biomass Combustion. *Environ Sci Technol* **2019,** *53* (4), 2209-2219.

47. Ngeno, G.; Otieno, N.; Troncoso, K.; Edwards, R. Opportunities for transition to clean household energy in Kenya: application of the WHO household energy assessment rapid tool (HEART). **2018**.

48. Mortimer, K.; Ndamala, C. B.; Naunje, A. W.; Malava, J.; Katundu, C.; Weston, W.; Havens, D.; Pope, D.; Bruce, N. G.; Nyirenda, M.; Wang, D.; Crampin, A.; Grigg, J.; Balmes, J.; Gordon, S. B. A cleaner burning biomass-fuelled cookstove intervention to prevent pneumonia in children under 5 years old in rural Malawi (the Cooking and Pneumonia Study): a cluster randomised controlled trial. *The Lancet* **2017,** *389* (10065), 167-175.

49. Chartier, R.; Phillips, M.; Mosquin, P.; Elledge, M.; Bronstein, K.; Nandasena, S.; Thornburg, V.; Thornburg, J.; Rodes, C. A comparative study of human exposures to household air pollution from commonly used cookstoves in Sri Lanka. *Indoor Air* **2017,** *27* (1), 147-159.

50. Grieshop, A. P.; Jain, G.; Sethuraman, K.; Marshall, J. D. Emission factors of health- and climate-relevant pollutants measured in home during a carbon-finance-approved cookstove intervention in rural India. *Geo. Health* **2017,** *1* (5), 222-236.

51. Reece, S. M.; Sinha, A.; Grieshop, A. P. Primary and photochemically aged aerosol emissions from biomass cookstoves: chemical and physical characterization. *Environ. Sci. Technol.* **2017**.

52. Saliba, G.; Subramanian, R.; Bilsback, K.; L'Orange, C.; Volckens, J.; Johnson, M.; Robinson, A. L. Aerosol Optical Properties and Climate Implications of Emissions from Traditional and Improved Cookstoves. *Environ. Sci. Technol.* **2018,** *52* (22), 13647-13656.

53. Preble, C. V.; Hadley, O. L.; Gadgil, A. J.; Kirchstetter, T. W. Emissions and climate-relevant optical properties of pollutants emitted from a three-stone fire and the Berkeley-Darfur stove tested under laboratory conditions. *Environ. Sci. Technol.* **2014,** *48* (11), 6484-91.

54. Arora, P.; Jain, S. Estimation of organic and elemental carbon emitted from wood burning in traditional and improved cookstoves using controlled cooking test. *Environ. Sci. Technol.* **2015,** *49* (6), 3958-65.

55. Hawley, B.; Volckens, J. Proinflammatory effects of cookstove emissions on human bronchial epithelial cells. *Indoor Air* **2013,** *23* (1), 4-13.

56. Gibbs-Flournoy, E. A.; Gilmour, M. I.; Higuchi, M.; Jetter, J.; George, I.; Copeland, L.; Harrison, R.; Moser, V. C.; Dye, J. A. Differential exposure and acute health impacts of inhaled solid-fuel emissions from rudimentary and advanced cookstoves in female CD-1 mice. *Environ. Res.* **2018,** *161*, 35-48.

57. Rosenthal, J.; Quinn, A.; Grieshop, A. P.; Pillarisetti, A.; Glass, R. I. Clean cooking and the SDGs: Integrated analytical approaches to guide energy interventions for health and environment goals. *Energy Sustain. Dev.* **2018,** *42*, 152-159.

58. Lacey, F. G.; Henze, D. K.; Lee, C. J.; van Donkelaar, A.; Martin, R. V. Transient climate and ambient health impacts due to national solid fuel cookstove emissions. *Proc. Natl. Acad. Sci. USA* **2017,** *114* (6), 1269-1274.
59. Shen, G.; Gaddam, C. K.; Ebersviller, S. M.; Vander Wal, R. L.; Williams, C.; Faircloth, J. W.; Jetter, J. J.; Hays, M. D. A Laboratory Comparison of Emission Factors, Number Size Distributions, and Morphology of Ultrafine Particles from 11 Different Household Cookstove-Fuel Systems. *Environ. Sci. Technol.* **2017,** *51* (11), 6522-6532.
60. Grieshop, A. P.; Marshall, J. D.; Kandlikar, M. Health and climate benefits of cookstove replacement options. *Energy Policy* **2011,** *39* (12), 7530-7542.
61. Puzzolo, E.; Pope, D.; Stanistreet, D.; Rehfuess, E. A.; Bruce, N. G. Clean fuels for resource-poor settings: A systematic review of barriers and enablers to adoption and sustained use. *Environ. Res.* **2016,** *146*, 218-34.
62. Mobarak, A. M.; Dwivedi, P.; Bailis, R.; Hildemann, L.; Miller, G. Low demand for nontraditional cookstove technologies. *Proc. Natl. Acad. Sci. USA* **2012,** *109* (27), 10815-20.
63. Faraday, M. The chemical history of a candle. *Resonance* **2002,** *7* (3), 90-98.
64. Pagels, J.; Wierzbicka, A.; Nilsson, E.; Isaxon, C.; Dahl, A.; Gudmundsson, A.; Swietlicki, E.; Bohgard, M. Chemical composition and mass emission factors of candle smoke particles. *J. Aerosol Sci.* **2009,** *40* (3), 193-208.
65. Fine, P. M.; Cass, G. R.; Simoneit, B. R. T. Characterization of Fine Particle Emissions from Burning Church Candles. *Environ. Sci. Technol.* **1999,** *33* (14), 2352-2362.
66. Zai, S.; Zhen, H.; Jia-song, W. Studies on the size distribution, number and mass emission factors of candle particles characterized by modes of burning. *J. Aerosol Sci.* **2006,** *37* (11), 1484-1496.
67. https://www.ecolabel.dk/-/criteriadoc/5371 accessed 15-03-2021.
68. Corley, R. H. V. How much palm oil do we need? *Environ. Sci. & Policy* **2009,** *12* (2), 134-139.
69. Fitzherbert, E. B.; Struebig, M. J.; Morel, A.; Danielsen, F.; Bruhl, C. A.; Donald, P. F.; Phalan, B. How will oil palm expansion affect biodiversity? *Trends. Ecol. Evol.* **2008,** *23* (10), 538-45.
70. Wang, Y.; Chung, S. H. Soot formation in laminar counterflow flames. *Prog. Energy Combust. Sci.* **2019,** *74*, 152-238.
71. Frenklach, M.; Wang, H. In *Detailed modeling of soot particle nucleation and growth*, Symposium (International) on Combustion, 1991; Citeseer: 1991; pp 1559-1566.
72. Frenklach, M. Reaction mechanism of soot formation in flames. *Phys. Chem. Chem. Phys.* **2002,** *4* (11), 2028-2037.
73. Thomsen, M. C.; Fuentes, A.; Demarco, R.; Volkwein, C.; Consalvi, J. L.; Reszka, P. Soot measurements in candle flames. *Exp. Therm. Fluid Sci.* **2017,** *82*, 116-123.
74. Mulay, M. R.; Chauhan, A.; Patel, S.; Balakrishnan, V.; Halder, A.; Vaish, R. Candle soot: Journey from a pollutant to a functional material. *Carbon* **2019,** *144*, 684-712.

75. Aronsson, U.; Chartier, C.; Andersson, Ö.; Johansson, B.; Sjöholm, J.; Wellander, R.; Richter, M.; Alden, M.; Miles, P. Analysis of EGR Effects on the Soot Distribution in a Heavy Duty Diesel Engine using Time-Resolved Laser Induced Incandescence. *SAE Int. J. Engines* **2010,** *3* (2), 137-155.

76. Sullivan, A. L.; Ball, R. Thermal decomposition and combustion chemistry of cellulosic biomass. *Atmos. Environ.* **2012,** *47*, 133-141.

77. Zadeh, Z. E.; Abdulkhani, A.; Aboelazayem, O.; Saha, B. Recent Insights into Lignocellulosic Biomass Pyrolysis: A Critical Review on Pretreatment, Characterization, and Products Upgrading. *Processes* **2020,** *8* (7), 799.

78. Simoneit, B. R., Schauer, J. J., Nolte, C. G., Oros, D. R., Elias, V. O., Fraser, M. P., Rogge, W.F. & Cass, G. R. Levoglucosan, a tracer for cellulose in biomass burning and atmospheric particles. *Atmos. Environ.* **1999,** *33* (2), 173-182.

79. Liu, W. J.; Li, W. W.; Jiang, H.; Yu, H. Q. Fates of Chemical Elements in Biomass during Its Pyrolysis. *Chem. Rev.* **2017**.

80. Sekimoto, K.; Koss, A. R.; Gilman, J. B.; Selimovic, V.; Coggon, M. M.; Zarzana, K. J.; Yuan, B.; Lerner, B. M.; Brown, S. S.; Warneke, C.; Yokelson, R. J.; Roberts, J. M.; de Gouw, J. High- and low-temperature pyrolysis profiles describe volatile organic compound emissions from western US wildfire fuels. *Atmos. Chem. Phys.* **2018,** *18* (13), 9263-9281.

81. Anca-Couce, A. Reaction mechanisms and multi-scale modelling of lignocellulosic biomass pyrolysis. *Prog. Energy Combust. Sci.* **2016,** *53*, 41-79.

82. McGrath, T. E.; Chan, W. G.; Hajaligol, M. R. Low temperature mechanism for the formation of polycyclic aromatic hydrocarbons from the pyrolysis of cellulose. *J. Anal. Appl. Pyrol.* **2003,** *66* (1-2), 51-70.

83. Milne, T. A.; Evans, R. J.; Abatzaglou, N. *Biomass gasifier"Tars": their nature, formation, and conversion*; National Renewable Energy Laboratory, Golden, CO (US): 1998.

84. Fitzpatrick, E. M.; Bartle, K. D.; Kubacki, M. L.; Jones, J. M.; Pourkashanian, M.; Ross, A. B.; Williams, A.; Kubica, K. The mechanism of the formation of soot and other pollutants during the co-firing of coal and pine wood in a fixed bed combustor. *Fuel* **2009,** *88* (12), 2409-2417.

85. Islam, M. M.; Wathore, R.; Zerriffi, H.; Marshall, J. D.; Bailis, R.; Grieshop, A. P. In-use emissions from biomass and LPG stoves measured during a large, multi-year cookstove intervention study in rural India. *Sci. Total Environ.* **2021,** *758*, 143698.

86. van Zyl, L.; Tryner, J.; Bilsback, K. R.; Good, N.; Hecobian, A.; Sullivan, A.; Zhou, Y.; Peel, J. L.; Volckens, J. Effects of Fuel Moisture Content on Emissions from a Rocket-Elbow Cookstove. *Environ. Sci. Technol.* **2019,** *53* (8), 4648-4656.

87. Schettler, T. Human exposure to phthalates via consumer products. *Int. J. Androl.* **2006,** *29* (1), 134-9; discussion 181-5.

88. Wormuth, M.; Scheringer, M.; Vollenweider, M.; Hungerbuhler, K. What are the sources of exposure to eight frequently used phthalic acid esters in Europeans? *Risk Anal.* **2006,** *26* (3), 803-24.

89. Frederiksen, H.; Jensen, T. K.; Jørgensen, N.; Kyhl, H. B.; Husby, S.; Skakkebæk, N. E.; Main, K. M.; Juul, A.; Andersson, A.-M. Human urinary

excretion of non-persistent environmental chemicals: an overview of Danish data collected between 2006 and 2012. *Reproduction* **2014,** *147* (4), 555-565.

90. Koch, H. M.; Ruther, M.; Schutze, A.; Conrad, A.; Palmke, C.; Apel, P.; Bruning, T.; Kolossa-Gehring, M. Phthalate metabolites in 24-h urine samples of the German Environmental Specimen Bank (ESB) from 1988 to 2015 and a comparison with US NHANES data from 1999 to 2012. *Int. J. Hyg. Environ. Health* **2017,** *220* (2 Pt A), 130-141.

91. Bu, S.; Wang, Y.; Wang, H.; Wang, F.; Tan, Y. Analysis of global commonly-used phthalates and non-dietary exposure assessment in indoor environment. *Building and Environment* **2020,** *177*.

92. Kay, V. R.; Bloom, M. S.; Foster, W. G. Reproductive and developmental effects of phthalate diesters in males. *Crit. Rev. Toxicol.* **2014,** *44* (6), 467-98.

93. Kay, V. R.; Chambers, C.; Foster, W. G. Reproductive and developmental effects of phthalate diesters in females. *Crit. Rev. Toxicol.* **2013,** *43* (3), 200-19.

94. Lyche, J. L.; Gutleb, A. C.; Bergman, Å.; Eriksen, G. S.; Murk, A. J.; Ropstad, E.; Saunders, M.; Skaare, J. U. Reproductive and developmental toxicity of phthalates. *J. Toxicol. Environ. Health, Part B* **2009,** *12* (4), 225-249.

95. Ernst, J.; Jann, J. C.; Biemann, R.; Koch, H. M.; Fischer, B. Effects of the environmental contaminants DEHP and TCDD on estradiol synthesis and aryl hydrocarbon receptor and peroxisome proliferator-activated receptor signalling in the human granulosa cell line KGN. *Mol. Hum. Reprod.* **2014,** *20* (9), 919-28.

96. Frederiksen, H.; Skakkebaek, N. E.; Andersson, A. M. Metabolism of phthalates in humans. *Mol. Nutr. Food Res.* **2007,** *51* (7), 899-911.

97. Manikkam, M.; Tracey, R.; Guerrero-Bosagna, C.; Skinner, M. K. Plastics derived endocrine disruptors (BPA, DEHP and DBP) induce epigenetic transgenerational inheritance of obesity, reproductive disease and sperm epimutations. *PLoS One* **2013,** *8* (1), e55387.

98. Bornehag, C.-G.; Sundell, J.; Weschler, C. J.; Sigsgaard, T.; Lundgren, B.; Hasselgren, M.; Hägerhed-Engman, L. The Association between Asthma and Allergic Symptoms in Children and Phthalates in House Dust: A Nested Case-Control Study. *Environ. Health Perspect.* **2004,** *112* (14), 1393-1397.

99. Whyatt, R. M.; Perzanowski, M. S.; Just, A. C.; Rundle, A. G.; Donohue, K. M.; Calafat, A. M.; Hoepner, L. A.; Perera, F. P.; Miller, R. L. Asthma in inner-city children at 5-11 years of age and prenatal exposure to phthalates: the Columbia Center for Children's Environmental Health Cohort. *Environ. Health Perspect.* **2014,** *122* (10), 1141-6.

100. Beko, G.; Callesen, M.; Weschler, C. J.; Toftum, J.; Langer, S.; Sigsgaard, T.; Host, A.; Kold Jensen, T.; Clausen, G. Phthalate exposure through different pathways and allergic sensitization in preschool children with asthma, allergic rhinoconjunctivitis and atopic dermatitis. *Environ. Res.* **2015,** *137*, 432-9.

101. Ipapo, K. N.; Factor-Litvak, P.; Whyatt, R. M.; Calafat, A. M.; Diaz, D.; Perera, F.; Rauh, V.; Herbstman, J. B. Maternal prenatal urinary phthalate metabolite concentrations and visual recognition memory among infants at 27 weeks. *Environ. Res.* **2017,** *155*, 7-14.

102. Olesen, T. S.; Bleses, D.; Andersen, H. R.; Grandjean, P.; Frederiksen, H.; Trecca, F.; Bilenberg, N.; Kyhl, H. B.; Dalsager, L.; Jensen, I. K.; Andersson, A. M.; Jensen, T. K. Prenatal phthalate exposure and language development in toddlers from the Odense Child Cohort. *Neurotoxicol. Teratol.* **2018,** *65*, 34-41.

103. Main, K. M.; Mortensen, G. K.; Kaleva, M. M.; Boisen, K. A.; Damgaard, I. N.; Chellakooty, M.; Schmidt, I. M.; Suomi, A.-M.; Virtanen, H. E.; Petersen, J. H.; Andersson, A.-M.; Toppari, J.; Skakkebæk, N. E. Human Breast Milk Contamination with Phthalates and Alterations of Endogenous Reproductive Hormones in Infants Three Months of Age. *Environ. Health Perspect.* **2006,** *114* (2), 270-276.

104. Mitro, S. D.; Johnson, T.; Zota, A. R. Cumulative Chemical Exposures During Pregnancy and Early Development. *Curr. Environ. Health Rep.* **2015,** *2* (4), 367-378.

105. Bornehag, C. G.; Carlstedt, F.; Jonsson, B. A.; Lindh, C. H.; Jensen, T. K.; Bodin, A.; Jonsson, C.; Janson, S.; Swan, S. H. Prenatal phthalate exposures and anogenital distance in Swedish boys. *Environ. Health Perspect.* **2015,** *123* (1), 101-7.

106. Dorman, D. C.; Chiu, W.; Hales, B. F.; Hauser, R.; Johnson, K. J.; Mantus, E.; Martel, S.; Robinson, K. A.; Rooney, A. A.; Rudel, R.; Sathyanarayana, S.; Schantz, S. L.; Waters, K. M. Systematic reviews and meta-analyses of human and animal evidence of prenatal diethylhexyl phthalate exposure and changes in male anogenital distance. *J. Toxicol. Environ. Health B. Crit. Rev.* **2018,** *21* (4), 207-226.

107. Xu, Y.; Liu, Z.; Park, J.; Clausen, P. A.; Benning, J. L.; Little, J. C. Measuring and predicting the emission rate of phthalate plasticizer from vinyl flooring in a specially-designed chamber. *Environ. Sci. Technol.* **2012,** *46* (22), 12534-41.

108. Clausen, P. A.; Liu, Z.; Kofoed-Sorensen, V.; Little, J.; Wolkoff, P. Influence of temperature on the emission of di-(2-ethylhexyl)phthalate (DEHP) from PVC flooring in the emission cell FLEC. *Environ. Sci. Technol.* **2012,** *46* (2), 909-15.

109. Ekelund, M.; Azhdar, B.; Gedde, U. W. Evaporative loss kinetics of di(2-ethylhexyl)phthalate (DEHP) from pristine DEHP and plasticized PVC. *Polym. Degrad. Stab.* **2010,** *95* (9), 1789-1793.

110. Christia, C.; Poma, G.; Harrad, S.; de Wit, C. A.; Sjostrom, Y.; Leonards, P.; Lamoree, M.; Covaci, A. Occurrence of legacy and alternative plasticizers in indoor dust from various EU countries and implications for human exposure via dust ingestion and dermal absorption. *Environ. Res.* **2019,** *171*, 204-212.

111. Silva, M. J.; Jia, T.; Samandar, E.; Preau, J. L., Jr.; Calafat, A. M. Environmental exposure to the plasticizer 1,2-cyclohexane dicarboxylic acid, diisononyl ester (DINCH) in U.S. adults (2000-2012). *Environ. Res.* **2013,** *126*, 159-63.

112. Frederiksen, H.; Nielsen, O.; Koch, H. M.; Skakkebaek, N. E.; Juul, A.; Jorgensen, N.; Andersson, A. M. Changes in urinary excretion of phthalates, phthalate substitutes, bisphenols and other polychlorinated and phenolic substances

in young Danish men; 2009-2017. *Int. J. Hyg. Environ. Health* **2020,** *223* (1), 93-105.

113. Pankow, J. F. An absorption model of gas/particle partitioning of organic compounds in the atmosphere. *Atmos. Environ.* **1994,** *28* (2), 185-188.

114. Schossler, P.; Schripp, T.; Salthammer, T.; Bahadir, M. Beyond phthalates: gas phase concentrations and modeled gas/particle distribution of modern plasticizers. *Sci. Total Environ.* **2011,** *409* (19), 4031-8.

115. Xu, Y.; Cohen Hubal, E. A.; Clausen, P. A.; Little, J. C. Predicting Residential Exposure to Phthalate Plasticizer Emitted from Vinyl Flooring: A Mechanistic Analysis. *Environ. Sci. Technol.* **2009,** *43* (7), 2374-2380.

116. Heyder, J.; Gebhart, J.; Rudolf, G.; Schiller, C. F.; Stahlhofen, W. Deposition of particles in the human respiratory tract in the size range 0.005–15 μm. *J. Aerosol Sci.* **1986,** *17* (5), 811-825.

117. Davies, C. N. Absorption of gases in the respiratory tract. *Ann. Occup. Hyg.* **1985,** *29* (1), 13-25.

118. Volckens, J.; Leith, D. Partitioning theory for respiratory deposition of semivolatile aerosols. *Ann. Occup. Hyg.* **2003,** *47* (2), 157-164.

119. Weschler, C. J.; Nazaroff, W. W. SVOC exposure indoors: fresh look at dermal pathways. *Indoor Air* **2012,** *22* (5), 356-77.

120. Shi, S.; Zhao, B. Modeled exposure assessment via inhalation and dermal pathways to airborne semivolatile organic compounds (SVOCs) in residences. *Environ. Sci. Technol.* **2014,** *48* (10), 5691-9.

121. Cao, J.; Weschler, C. J.; Luo, J.; Zhang, Y. C(m)-History Method, a Novel Approach to Simultaneously Measure Source and Sink Parameters Important for Estimating Indoor Exposures to Phthalates. *Environ. Sci. Technol.* **2016,** *50* (2), 825-34.

122. Isaxon, C.; Dierschke, K.; Pagels, J.; Löndahl, J.; Gudmundsson, A.; Hagerman, I.; Berglund, M.; Wierzbicka, A.; Assarsson, E.; Andersson, U. B.; Jönsson, B. A. G.; Messing, M. E.; Nielsen, J.; Bohgard, M. A Novel System for Source Characterization and Controlled Human Exposure to Nanoparticle Aggregates Generated During Gas–Metal Arc Welding. *Aerosol Sci. Technol.* **2013,** *47* (1), 52-59.

123. Rasmussen, B. B.; Wang, K.; Karstoft, J. G.; Skov, S. N.; Kocks, M.; Andersen, C.; Wierzbicka, A.; Pagels, J.; Pedersen, P. B.; Glasius, M.; Bilde, M. Emissions of ultrafine particles from five types of candles during steady burn conditions. *Indoor Air* **2021**.

124. Wu, Y.; Cox, S. S.; Xu, Y.; Liang, Y.; Won, D.; Liu, X.; Clausen, P. A.; Rosell, L.; Benning, J. L.; Zhang, Y.; Little, J. C. A reference method for measuring emissions of SVOCs in small chambers. *Build. Environ.* **2016,** *95*, 126-132.

125. Weschler, C. J.; Beko, G.; Koch, H. M.; Salthammer, T.; Schripp, T.; Toftum, J.; Clausen, G. Transdermal Uptake of Diethyl Phthalate and Di(n-butyl) Phthalate Directly from Air: Experimental Verification. *Environ. Health Perspect.* **2015,** *123* (10), 928-34.

126. Nagy, A. Characterization of a new type of nanoparticle generator for medical inhalation applications (Master's Thesis). Retreived from https://lup.lub.lu.se/student-papers/search/publication/9024210. **2020**.

127. DeCarlo, P. F.; Kimmel, J. R.; Trimborn, A.; Northway, M. J.; Jayne, J. T.; Aiken, A. C.; Gonin, M.; Fuhrer, K.; Horvath, T.; Docherty, K. S. Field-deployable, high-resolution, time-of-flight aerosol mass spectrometer. *Anal. Chem.* **2006,** *78* (24), 8281-8289.

128. Canagaratna, M. R.; Jayne, J. T.; Jimenez, J. L.; Allan, J. D.; Alfarra, M. R.; Zhang, Q.; Onasch, T. B.; Drewnick, F.; Coe, H.; Middlebrook, A.; Delia, A.; Williams, L. R.; Trimborn, A. M.; Northway, M. J.; DeCarlo, P. F.; Kolb, C. E.; Davidovits, P.; Worsnop, D. R. Chemical and microphysical characterization of ambient aerosols with the aerodyne aerosol mass spectrometer. *Mass Spectrom. Rev.* **2007,** *26* (2), 185-222.

129. Onasch, T. B.; Trimborn, A.; Fortner, E. C.; Jayne, J. T.; Kok, G. L.; Williams, L. R.; Davidovits, P.; Worsnop, D. R. Soot Particle Aerosol Mass Spectrometer: Development, Validation, and Initial Application. *Aerosol Sci. Technol.* **2012,** *46* (7), 804-817.

130. Matthew, B. M.; Middlebrook, A. M.; Onasch, T. B. Collection Efficiencies in an Aerodyne Aerosol Mass Spectrometer as a Function of Particle Phase for Laboratory Generated Aerosols. *Aerosol Sci. Technol.* **2008,** *42* (11), 884-898.

131. Allan, J. D.; Jimenez, J. L.; Williams, P. I.; Alfarra, M. R.; Bower, K. N.; Jayne, J. T.; Coe, H.; Worsnop, D. R. Quantitative sampling using an Aerodyne aerosol mass spectrometer 1. Techniques of data interpretation and error analysis. *J. Geophys. Res. Atmospheres* **2003,** *108* (D3), n/a-n/a.

132. Elsasser, M.; Crippa, M.; Orasche, J.; DeCarlo, P. F.; Oster, M.; Pitz, M.; Cyrys, J.; Gustafson, T. L.; Pettersson, J. B. C.; Schnelle-Kreis, J.; Prévôt, A. S. H.; Zimmermann, R. Organic molecular markers and signature from wood combustion particles in winter ambient aerosols: aerosol mass spectrometer (AMS) and high time-resolved GC-MS measurements in Augsburg, Germany. *Atmos. Chem. Phys.* **2012,** *12* (14), 6113-6128.

133. Li, Y. J.; Yeung, J. W. T.; Leung, T. P. I.; Lau, A. P. S.; Chan, C. K. Characterization of Organic Particles from Incense Burning Using an Aerodyne High-Resolution Time-of-Flight Aerosol Mass Spectrometer. *Aerosol Sci. Technol.* **2012,** *46* (6), 654-665.

134. Herring, C. L.; Faiola, C. L.; Massoli, P.; Sueper, D.; Erickson, M. H.; McDonald, J. D.; Simpson, C. D.; Yost, M. G.; Jobson, B. T.; VanReken, T. M. New Methodology for Quantifying Polycyclic Aromatic Hydrocarbons (PAHs) Using High-Resolution Aerosol Mass Spectrometry. *Aerosol Sci. Technol.* **2015,** *49* (11), 1131-1148.

135. Xu, W.; Lambe, A.; Silva, P.; Hu, W.; Onasch, T.; Williams, L.; Croteau, P.; Zhang, X.; Renbaum-Wolff, L.; Fortner, E.; Jimenez, J. L.; Jayne, J.; Worsnop, D.; Canagaratna, M. Laboratory evaluation of species-dependent relative ionization efficiencies in the Aerodyne Aerosol Mass Spectrometer. *Aerosol. Sci. Technol.* **2018**, 1-16.

136. Malmborg, V. B.; Eriksson, A. C.; Török, S.; Zhang, Y.; Kling, K.; Martinsson, J.; Fortner, E. C.; Gren, L.; Kook, S.; Onasch, T. B.; Bengtsson, P.-E.; Pagels, J. Relating aerosol mass spectra to composition and nanostructure of soot particles. *Carbon* **2019,** *142,* 535-546.
137. Zhang, J.; Smith, K.; Ma, Y.; Ye, S.; Jiang, F.; Qi, W.; Liu, P.; Khalil, M.; Rasmussen, R.; Thorneloe, S. Greenhouse gases and other airborne pollutants from household stoves in China: a database for emission factors. *Atmos. Environ.* **2000,** *34* (26), 4537-4549.
138. He, C., Morawska, L., Hitchins, J., & Gilbert, D Contribution from indoor sources to particle number and mass concentrations in residential houses. *Atmos. Environ.* **2004,** *38* (21), 3405-3415.
139. Bergh, C.; Torgrip, R.; Emenius, G.; Ostman, C. Organophosphate and phthalate esters in air and settled dust - a multi-location indoor study. *Indoor Air* **2011,** *21* (1), 67-76.
140. Wang, S.; Dai, G.; Yang, H.; Luo, Z. Lignocellulosic biomass pyrolysis mechanism: A state-of-the-art review. *Prog. Energy Combust. Sci.* **2017,** *62,* 33-86.
141. Bobba, M. K.; Musculus, M. P. B. Laser diagnostics of soot precursors in a heavy-duty diesel engine at low-temperature combustion conditions. *Combustion and Flame* **2012,** *159* (2), 832-843.
142. Just, B.; Rogak, S.; Kandlikar, M. Characterization of ultrafine particulate matter from traditional and improved biomass cookstoves. *Environ. Sci. Technol.* **2013,** *47* (7), 3506-12.
143. de la Sota, C.; Lumbreras, J.; Pérez, N.; Ealo, M.; Kane, M.; Youm, I.; Viana, M. Indoor air pollution from biomass cookstoves in rural Senegal. *Energy Sustain. Dev.* **2018,** *43,* 224-234.
144. Zhu, Y.; Luo, M.; Ouyang, Q.; Huang, L.; Cao, B. Dynamic characteristics and comfort assessment of airflows in indoor environments: A review. *Build. Environ.* **2015,** *91,* 5-14.
145. Manoukian, A.; Quivet, E.; Temime-Roussel, B.; Nicolas, M.; Maupetit, F.; Wortham, H. Emission characteristics of air pollutants from incense and candle burning in indoor atmospheres. *Environ. Sci. Pollut. Res.* **2013,** *20* (7), 4659-4670.
146. Klosterköther, A.; Kurtenbach, R.; Wiesen, P.; Kleffmann, J. Determination of the emission indices for NO, NO2, HONO, HCHO, CO, and particles emitted from candles. *Indoor Air* **2020**.
147. Wallace, L.; Jeong, S. G.; Rim, D. Dynamic behavior of indoor ultrafine particles (2.3-64 nm) due to burning candles in a residence. *Indoor Air* **2019**.
148. Stabile, L.; Fuoco, F. C.; Buonanno, G. Characteristics of particles and black carbon emitted by combustion of incenses, candles and anti-mosquito products. *Build. Environ.* **2012,** *56,* 184-191.
149. Derudi, M.; Gelosa, S.; Sliepcevich, A.; Cattaneo, A.; Cavallo, D.; Rota, R.; Nano, G. Emission of air pollutants from burning candles with different composition in indoor environments. *Environ. Sci. Pollut. Res. Int.* **2014,** *21* (6), 4320-30.
150. Mohr, C.; Huffman, J. A.; Cubison, M. J.; Aiken, A. C.; Docherty, K. S.; Kimmel, J. R.; Ulbrich, I. M.; Hannigan, M.; Jimenez, J. L. Characterization of

Primary Organic Aerosol Emissions from Meat Cooking, Trash Burning, and Motor Vehicles with High-Resolution Aerosol Mass Spectrometry and Comparison with Ambient and Chamber Observations. *Environ. Sci. Technol.* **2009,** *43* (7), 2443-2449.

151. DeCarlo, P. F.; Avery, A. M.; Waring, M. S. Thirdhand smoke uptake to aerosol particles in the indoor environment. *Sci. Adv.* **2018,** *4* (5).

152. Lunderberg, D. M.; Kristensen, K.; Liu, Y.; Misztal, P. K.; Tian, Y.; Arata, C.; Wernis, R.; Kreisberg, N.; Nazaroff, W. W.; Goldstein, A. H. Characterizing Airborne Phthalate Concentrations and Dynamics in a Normally Occupied Residence. *Environ. Sci. Technol.* **2019,** *53* (13), 7337-7346.

153. Lunderberg, D. M.; Kristensen, K.; Tian, Y.; Arata, C.; Misztal, P. K.; Liu, Y.; Kreisberg, N.; Katz, E. F.; DeCarlo, P. F.; Patel, S.; Vance, M. E.; Nazaroff, W. W.; Goldstein, A. H. Surface Emissions Modulate Indoor SVOC Concentrations through Volatility-Dependent Partitioning. *Environ. Sci. Technol.* **2020,** *54* (11), 6751-6760.

154. National Institute for Public Health and the Environment (RIVM) (2002). Multiple Path Particle Dosimetry Model (MPPD v 1.0): A Model for Human and Rat Airway Particle Dosimetry. Bilthoven, The Netherlands. RIVA Report 650010030.

155. Roldin, P.; Eriksson, A. C.; Nordin, E. Z.; Hermansson, E.; Mogensen, D.; Rusanen, A.; Boy, M.; Swietlicki, E.; Svenningsson, B.; Zelenyuk, A.; Pagels, J. Modelling non-equilibrium secondary organic aerosol formation and evaporation with the aerosol dynamics, gas- and particle-phase chemistry kinetic multilayer model ADCHAM. *Atmos. Chem. Phys.* **2014,** *14* (15), 7953-7993.

156. Vaden, T. D.; Imre, D.; Beranek, J.; Shrivastava, M.; Zelenyuk, A. Evaporation kinetics and phase of laboratory and ambient secondary organic aerosol. *Proc. Natl. Acad. Sci. USA* **2011,** *108* (6), 2190-5.

157. Krais, A. M.; Andersen, C.; Eriksson, A. C.; Johnsson, E.; Nielsen, J.; Pagels, J.; Gudmundsson, A.; Lindh, C. H.; Wierzbicka, A. Excretion of Urinary Metabolites of the Phthalate Esters DEP and DEHP in 16 Volunteers after Inhalation and Dermal Exposure. *Int. J. Environ. Res. Public Health* **2018,** *15* (11).

158. Beko, G.; Morrison, G.; Weschler, C. J.; Koch, H. M.; Palmke, C.; Salthammer, T.; Schripp, T.; Eftekhari, A.; Toftum, J.; Clausen, G. Dermal uptake of nicotine from air and clothing: Experimental verification. *Indoor Air* **2018,** *28* (2), 247-257.

159. Blanchard, O.; Glorennec, P.; Mercier, F.; Bonvallot, N.; Chevrier, C.; Ramalho, O.; Mandin, C.; Bot, B. L. Semivolatile organic compounds in indoor air and settled dust in 30 French dwellings. *Environ. Sci. Technol.* **2014,** *48* (7), 3959-3969.

160. Li, H. L.; Ma, W. L.; Liu, L. Y.; Zhang, Z.; Sverko, E.; Zhang, Z. F.; Song, W. W.; Sun, Y.; Li, Y. F. Phthalates in infant cotton clothing: Occurrence and implications for human exposure. *Sci. Total Environ.* **2019,** *683*, 109-115.

161. Morrison, G.; Li, H.; Mishra, S.; Buechlein, M. Airborne phthalate partitioning to cotton clothing. *Atmos. Environ.* **2015,** *115*, 149-152.

162. Gong, M.; Weschler, C. J.; Zhang, Y. Impact of Clothing on Dermal Exposure to Phthalates: Observations and Insights from Sampling Both Skin and Clothing. *Environ. Sci. Technol.* **2016,** *50* (8), 4350-7.

163. Organization, W. H., *WHO guidelines for indoor air quality: household fuel combustion*. World Health Organization: 2014.

164. Lewne, M.; Johannesson, S.; Strandberg, B.; Bigert, C. Exposure to Particles, Polycyclic Aromatic Hydrocarbons, and Nitrogen Dioxide in Swedish Restaurant Kitchen Workers. *Ann. Work Expo. Health* **2017,** *61* (2), 152-163.

165. Bohlin, P.; Jones, K. C.; Tovalin, H.; Strandberg, B. Observations on persistent organic pollutants in indoor and outdoor air using passive polyurethane foam samplers. *Atmospheric Environment* **2008,** *42* (31), 7234-7241.

166. Klingberg, J.; Broberg, M.; Strandberg, B.; Thorsson, P.; Pleijel, H. Influence of urban vegetation on air pollution and noise exposure - A case study in Gothenburg, Sweden. *Sci. Total Environ.* **2017,** *599-600*, 1728-1739.

167. Gustafson, P.; Östman, C.; Sällsten, G. Indoor Levels of Polycyclic Aromatic Hydrocarbons in Homes with or without Wood Burning for Heating. *Environ. Sci. Technol.* **2008,** *42* (14), 5074-5080.

168. Dons, E.; Int Panis, L.; Van Poppel, M.; Theunis, J.; Willems, H.; Torfs, R.; Wets, G. Impact of time–activity patterns on personal exposure to black carbon. *Atmos. Environ.* **2011,** *45* (21), 3594-3602.

169. Merritt, A. S.; Georgellis, A.; Andersson, N.; Bero Bedada, G.; Bellander, T.; Johansson, C. Personal exposure to black carbon in Stockholm, using different intra-urban transport modes. *Sci. Total Environ.* **2019,** *674*, 279-287.

170. Skovmand, A.; Damiao Gouveia, A. C.; Koponen, I. K.; Moller, P.; Loft, S.; Roursgaard, M. Lung inflammation and genotoxicity in mice lungs after pulmonary exposure to candle light combustion particles. *Toxicol. Lett.* **2017,** *276*, 31-38.

171. Damiao Gouveia, A. C.; Skovman, A.; Jensen, A.; Koponen, I. K.; Loft, S.; Roursgaard, M.; Moller, P. Telomere shortening and aortic plaque progression in Apoliprotein E knockout mice after pulmonary exposure to candle light combustion particles. *Mutagenesis* **2018**.

172. Shehab, M. A.; Pope, F. D. Effects of short-term exposure to particulate matter air pollution on cognitive performance. *Sci. Rep.* **2019,** *9* (1).

173. Soppa, V. J.; Schins, R. P.; Hennig, F.; Hellack, B.; Quass, U.; Kaminski, H.; Kuhlbusch, T. A.; Hoffmann, B.; Weinmayr, G. Respiratory effects of fine and ultrafine particles from indoor sources--a randomized sham-controlled exposure study of healthy volunteers. *Int. J. Environ. Res. Public Health* **2014,** *11* (7), 6871-89.

Printed by Media-Tryck, Lund 2021 NORDIC SWAN ECOLABEL 3041 0903

LUND
UNIVERSITY

Ergonomics and Aerosol Technology
Department of Design Sciences
Faculty of Engineering, Lund University

ISSN 1650-9773, Publication 69
ISBN 978-91-7895-810-8

9 789178 958108